activity was examined by the luciferase assay (A, C), and cell viability was measured by the WST-8 assay (B, D). The data represent the mean of three experiments, and the bars indicate S.D. values. The western blot analysis (E) and relative intensity of HCV-NS5B protein band was measured by LAS3000 and normalized with that of actin (F) after the treatment with siRNAs targeted against DHCR24 (siDHCR24-417 and 1024) or HCV (siE-R7) in FLR3-1 replicon cells. (G, H) In HCV JFH-1-infected cells, DHCR24 knockdown by siDHCR24-417 and 1024 and HCV knockdown by siE-R7 were performed, and DHCR24 and HCV core protein expression was confirmed by western blot analysis. Relative intensity ratio of core protein to actin was indicated (H). The data represent the mean of three experiments, and the bars indicate S.D. values. *P<0.05, **P<0.01(two-tailed Student's t-test).

Fig. 3. The level of cholesterol and DHCR24 expression.

(A) Cholesterol synthesis pathway, starting from HMG-CoA [26]. The abbreviations used are: D8D7I, 3 β hydroxysterol-delta8-delta7-isomerase; and C5DS, 3 β hydroxysterol-C^5-desaturase. (B) Cholesterol (0, 100, and 200 μg/ml) was added to HuH-7 cells, and, after 24 hours, DHCR24 protein was detected by western blot analysis using anti-DHCR24 MoAb and protein band intensity was measured and normalized with that of actin (lower column). (C) HepG2 cells were treated with MβCD (0, 1.25, 2.5, 5, and 10 mM) for 30 minutes. After 72 hours, these cells were harvested and examined by western blot analysis with the anti-DHCR24 MoAb and relative intensity was measured as described in (B)(lower column). (D) Cholesterol concentration in R6FLR-N cells was measured after treatment with non-targeting

ACCEPTED MANUSCRIPT

siRNA and DHCR24 siRNA (417 and 1024). The cholesterol contents were measured by Amplex Red cholesterol assay, plotted based on fluorescence units and were normalized against actin which was measured by western blot analysis, and the relative ratio was then calculated. The data represent the mean of three experiments, and the bars indicate the S.D. values.

Fig. 4. Effect of U18666A on HCV replication

(A) Addition of U18666A to FLR3-1 cells and subsequent examination of HCV replication by the luciferase assay. Cell viability was measured by WST-8 assay. HCV replication and cell viability were measured 48 hours after addition of U18666A. The bars indicate S.D. values. Open diamonds indicate the relative ratio of viral replication, and black squares indicate the cell viability in relation to the untreated controls (A, C-E). (B) Treatment of FLR3-1 cells with U18666A decreased the expression of HCV proteins in a dose-dependent manner, as determined by western blot analysis. (C-D) Effect of U18666A on HCV replication in other HCV replicon cells (C, R6FLR-N cells; D, Rep JFH Luc 3-13 cells). HCV replication and cell viability analyses were performed as described above. (E) The effect of the DHCR7 inhibitor BD1008 on HCV replicon cells (FLR3-1). Replication activity was examined by the luciferase assay, and cell viability was measured by the WST-8 assay. HCV replication and cell viability analyses were performed 48 hours after the addition of U18666A. (F-G) FLR3-1 cells ($5x10^3$ cells/well) were treated with U18666A alone (open square), low density lipoprotein (LDL) (final cholesterol concentration, 50 μg/ml), and U18666A (gray square). HCV replication was determined by the luciferase assay 48 hours later (F), and cell viability was measured by the WST-8 assay (G). *p<0.05 (two-tailed Student's t-test). The data

represent the mean of three experiments, and the bars indicate S.D. values.

Fig. 5. Effect of U18666A on cells infected with HCV JFH-1.

HCV JFH-1-infected cells treated with U18666A were examined 72 hours after treatment. (A) Expression of HCV-NS5B protein with or without U18666A treatment, as confirmed by western blot analysis. (B) The intensity of HCV-NS5B protein expression represented graphically. (C) HCV RNA in HCV JFH-1-infected cells with or without U18666A treatment was measured by RTD-PCR as described in the Materials and methods. (D) Cell viability was measured by the WST-8 assay.

Fig. 6. Evaluation of the anti-HCV effect of U18666A in chimeric mice.

(A) The schedule that was followed to produce chimeric mice with humanized liver, perform blood sampling, and administer drugs to chimeric mice infected with HCV. Four groups of three chimeric mice with humanized liver each were treated intraperitoneally with U18666A (10 mg/kg) and/or subcutaneously with PEG-IFN (30 μg/kg) at 2-day intervals for 2 weeks. (B) The effect of U18666A and/or PEG-IFN on HCV replication in chimeric mice with humanized liver was determined by quantification of HCV-RNA using RTD-PCR. The bars indicate S.D. values (n=12). (C) Human albumin concentrations in the sera of chimeric mice with humanized liver. The bars indicate S.D. values (n=12).

ACCEPTED MANUSCRIPT

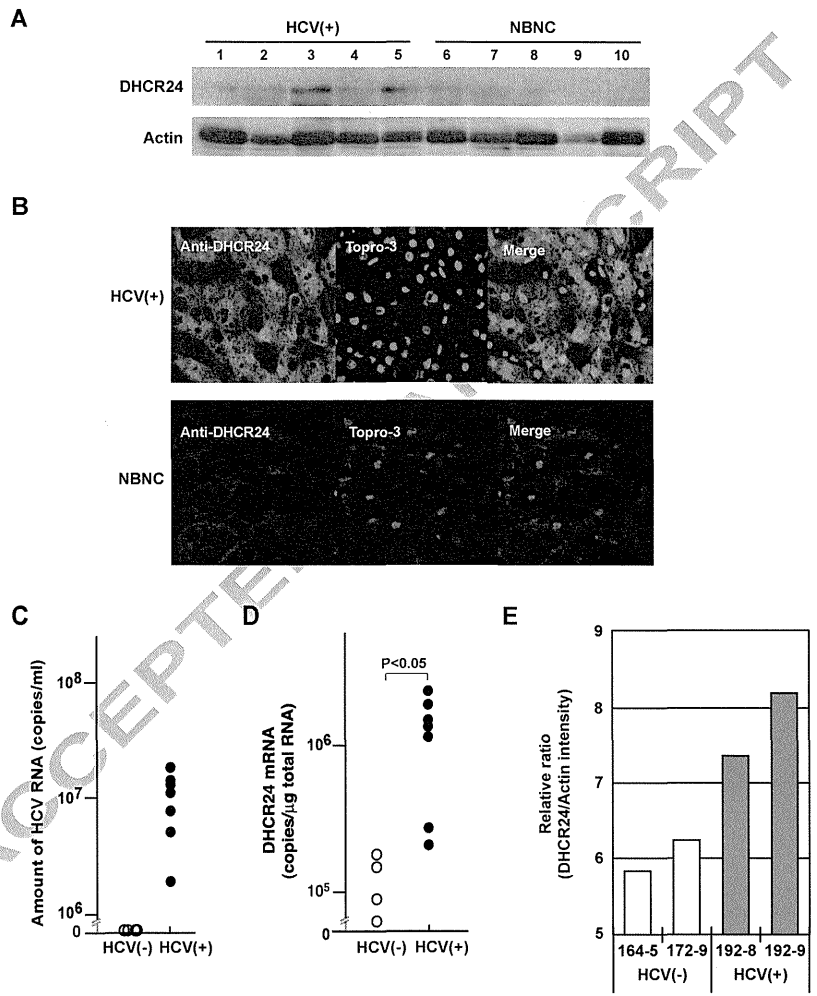

Fig.1 Takano et al.

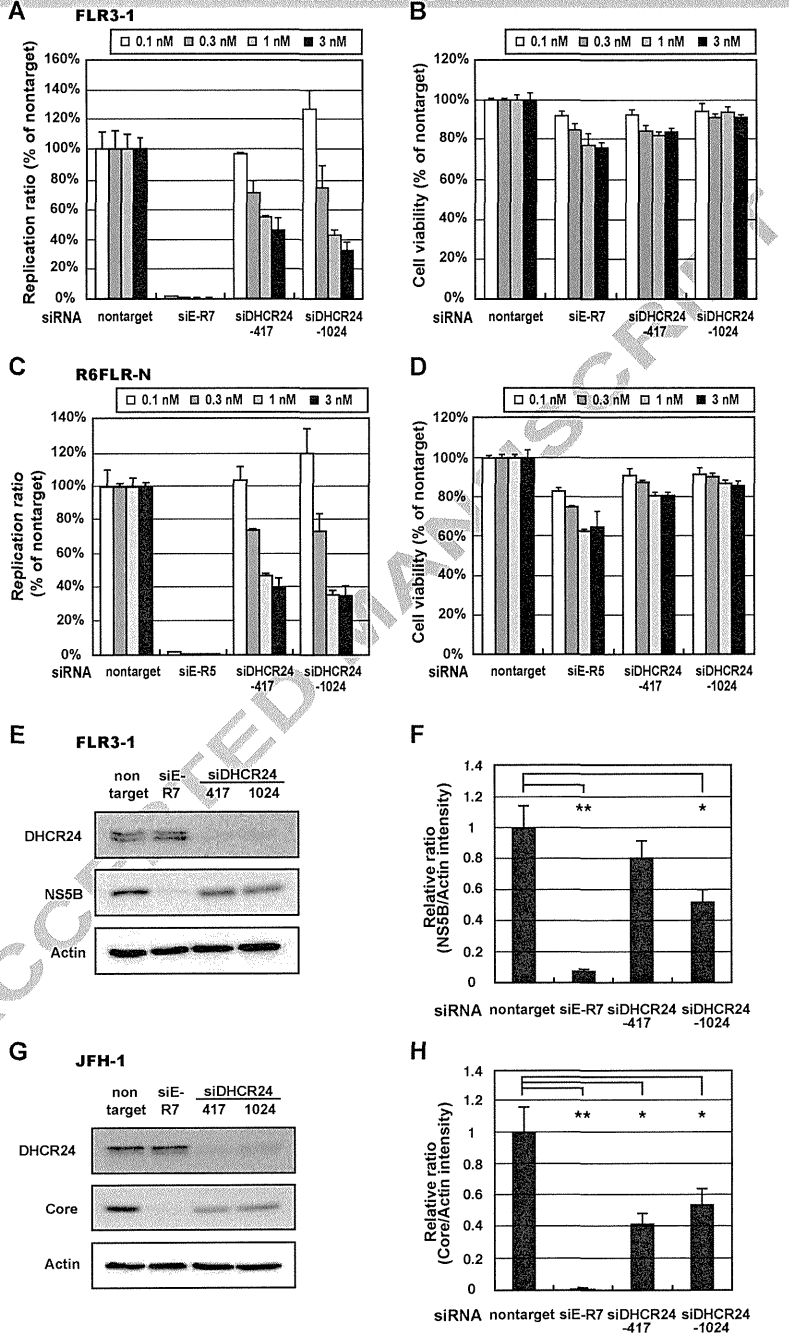

Fig. 2 Takano et al.

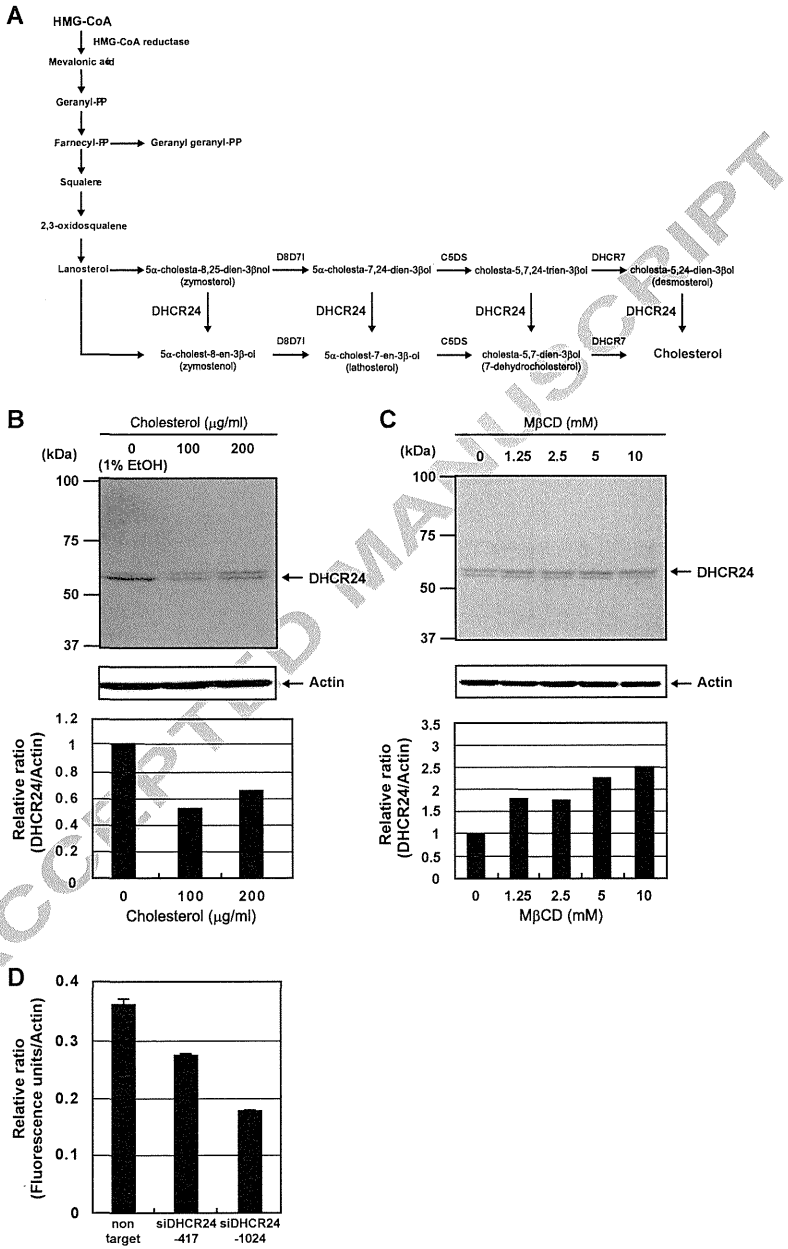

Fig. 3 Takano et al.

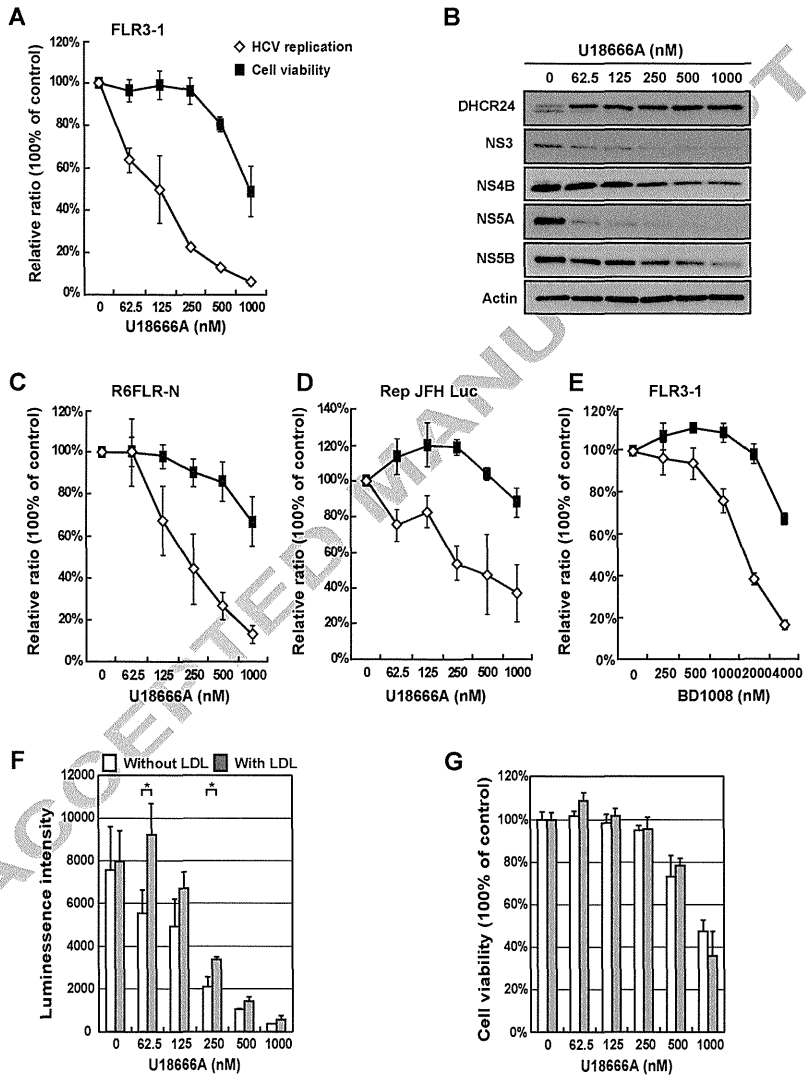

Fig.4 Takano et al.

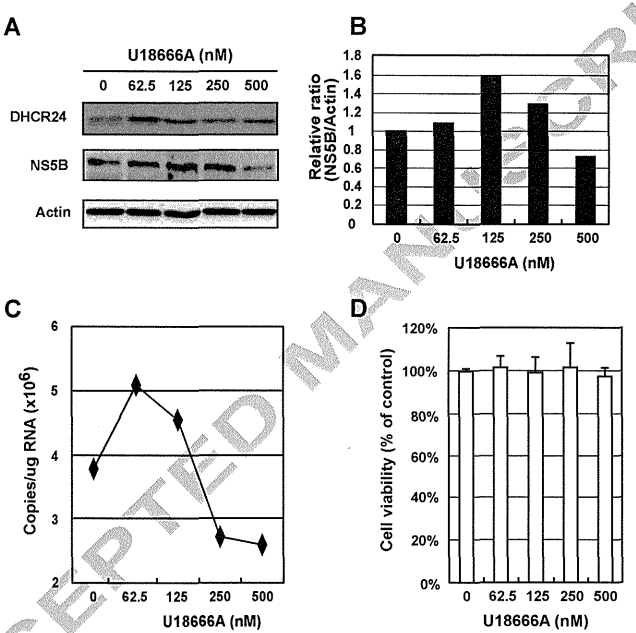

Fig. 5 Takano et al.

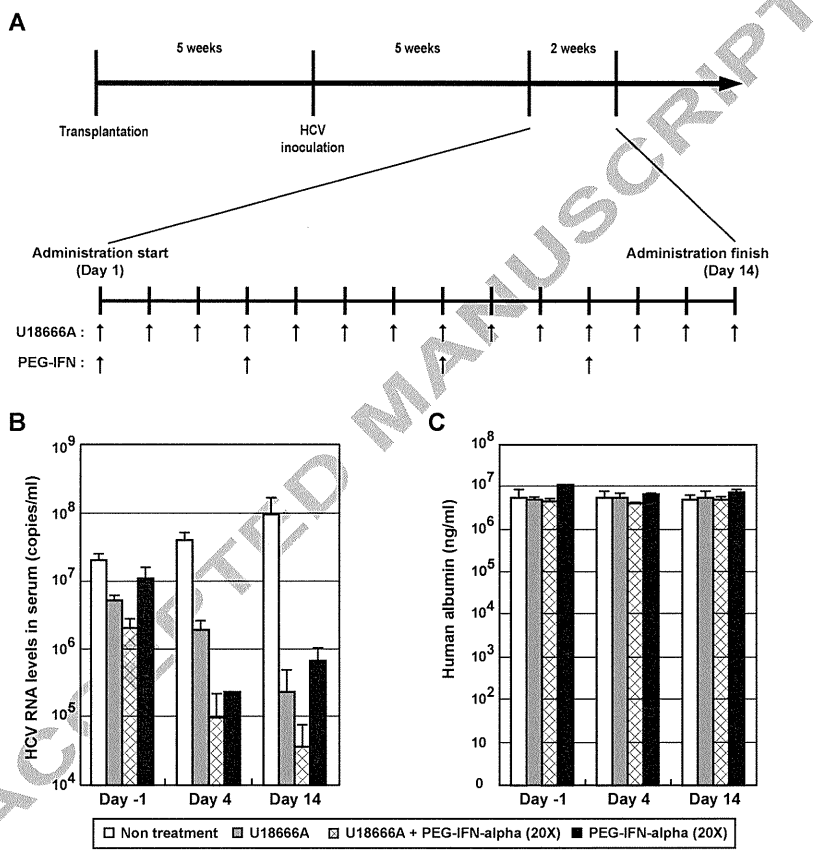

Fig. 6 Takano et al.

Persistent expression of the full genome of hepatitis C virus in B cells induces spontaneous development of B-cell lymphomas in vivo

*Yuri Kasama,[1] *Satoshi Sekiguchi,[2] Makoto Saito,[1] Kousuke Tanaka,[1] Masaaki Satoh,[1] Kazuhiko Kuwahara,[3] Nobuo Sakaguchi,[3] Motohiro Takeya,[4] Yoichi Hiasa,[5] Michinori Kohara,[2] and Kyoko Tsukiyama-Kohara[1]

[1]Department of Experimental Phylaxiology, Faculty of Life Sciences, Kumamoto University, Kumamoto, Japan; [2]Department of Microbiology and Cell Biology, Tokyo Metropolitan Institute of Medical Science, Tokyo, Japan; [3]Department of Immunology, Faculty of Life Sciences, Kumamoto University, Kumamoto, Japan; [4]Department of Cell Pathology, Faculty of Life Sciences, Kumamoto University, Kumamoto, Japan; and [5]Department of Gastroenterology and Metabology, Ehime University Graduate School of Medicine, To-on, Ehime, Japan

Extrahepatic manifestations of hepatitis C virus (HCV) infection occur in 40%-70% of HCV-infected patients. B-cell non-Hodgkin lymphoma is a typical extrahepatic manifestation frequently associated with HCV infection. The mechanism by which HCV infection of B cells leads to lymphoma remains unclear. Here we established HCV transgenic mice that express the full HCV genome in B cells (RzCD19Cre mice) and observed a 25.0% incidence of diffuse large B-cell non-Hodgkin lymphomas (22.2% in males and 29.6% in females) within 600 days after birth. Expression levels of aspartate aminotransferase and alanine aminotransferase, as well as 32 different cytokines, chemokines and growth factors, were examined. The incidence of B-cell lymphoma was significantly correlated with only the level of soluble interleukin-2 receptor α subunit (sIL-2Rα) in RzCD19Cre mouse serum. All RzCD19Cre mice with substantially elevated serum sIL-2Rα levels (> 1000 pg/mL) developed B-cell lymphomas. Moreover, compared with tissues from control animals, the B-cell lymphoma tissues of RzCD19Cre mice expressed significantly higher levels of IL-2Rα. We show that the expression of HCV in B cells promotes non-Hodgkin–type diffuse B-cell lymphoma, and therefore, the RzCD19Cre mouse is a powerful model to study the mechanisms related to the development of HCV-associated B-cell lymphoma. (*Blood*. 2010;116(23):4926-4933)

Introduction

More than 175 million people worldwide are infected with hepatitis C virus (HCV), a positive-strand RNA virus that infects both hepatocytes and peripheral blood mononuclear cells.[1] Chronic HCV infection may lead to hepatitis, liver cirrhosis, hepatocellular carcinomas[2,3] and lymphoproliferative diseases such as B-cell non-Hodgkin lymphoma and mixed-cryoglobulinemia.[1,4-6] B-cell non-Hodgkin lymphoma is a typical extrahepatic manifestation frequently associated with HCV infection[7] with geographic and ethnic variability.[8,9] Based on a meta-analysis, the prevalence of HCV infection in patients with B-cell non-Hodgkin lymphoma is approximately 15%.[8] The HCV envelope protein E2 binds human CD81,[10] a tetraspanin expressed on various cell types including lymphocytes, and activates B-cell proliferation[11]; however, the precise mechanism of disease onset remains unclear. We previously developed a transgenic mouse model that conditionally expresses HCV cDNA (nucleotides 294-3435), including the viral genes that encode the core, E1, E2, and NS2 proteins, using the Cre/*lox*P system (in core~NS2 [CN2] mice).[12,13] The conditional transgene activation of the HCV cDNA (core, E1, E2, and NS2) protects mice from Fas-mediated lethal acute liver failure by inhibiting cytochrome c release from mitochondria.[13] In HCV-infected mice, persistent HCV protein expression is established by targeted disruption of *irf-1*, and high incidences of lymphoproliferative disorders are found in CN2 *irf-1*$^{-/-}$ mice.[14] Infection and replication of HCV also occur in B cells,[15,16] although the direct effects, particularly in vivo, of HCV infection on B cells have not been clarified.

To define the direct effect of HCV infection on B cells in vivo, we crossed transgenic mice with an integrated full-length HCV genome (Rz) under the conditional Cre/*lox*P expression system with mice expressing the Cre enzyme under transcriptional control of the B lineage–restricted gene *CD19*,[17] we addressed the effects of HCV transgene expression in this study.

Methods

Animal experiments

Wild-type (WT), Rz, CD19Cre, RzCD19Cre mice (129/sv, BALB/c, and C57BL/6J mixed background), and MxCre/CN2-29 mice (C57BL/6J background) were maintained in conventional animal housing under specific pathogen-free conditions. All animal experiments were performed according to the guidelines of the Tokyo Metropolitan Institute of Medical Science or the Kumamoto University Subcommittee for Laboratory Animal Care. The protocol was approved by the Institutional Review Boards of both facilities.

Measurements of HCV protein and RNA

Mice were anesthetized and bled, and tissues (spleen, lymph nodes, liver, and tumors) were homogenized in lysis buffer (1% sodium dodecyl sulfate; 0.5% (wt/vol) nonyl phenoxypolyethoxylethanol; 0.15M NaCl; 10 mM

Submitted May 2, 2010; accepted August 13, 2010. Prepublished online as *Blood* First Edition paper, August 23, 2010; DOI 10.1182/blood-2010-05-283358.

*Y.K. and S.S. contributed equally to this work.

The online version of this article contains a data supplement.

The publication costs of this article were defrayed in part by page charge payment. Therefore, and solely to indicate this fact, this article is hereby marked "advertisement" in accordance with 18 USC section 1734.

tris(hydroxymethyl)aminomethane, pH 7.4) using a Dounce homogenizer. The concentration of HCV core protein in tissue lysates was measured using an HCV antigen enzyme-linked immunosorbent assay (ELISA; Ortho).[18] HCV mRNA was isolated by a guanidine thiocyanate protocol using ISOGEN (Nippon Gene) and was detected by reverse transcription polymerase chain reaction (RT-PCR) amplification using primers specific for the 5′ untranslated region of the *HCR6* sequence.[19,20] Reverse transcription was performed using Superscript III reverse transcriptase (Invitrogen) with random primers. PCR primers NCR-F (5′-TTCACGCAGAAAGCGTCTAGCCAT-3′) and NCR-R (5′-TCGTCCTGGCAATTCCGGTGTACT-3′) were used for the first round of HCV cDNA amplification, and the resulting product was used as a template for a second round of amplification using primers NCR-F INNER (5′-TTCCGCAGACCACTATGGCT-3′) and NCR-R INNER (5′-TTCCGCAGACCACTATGGCT-3′).

Collection of serum for chemokine ELISA

Blood samples were collected from the supraorbital veins or by heart puncture of killed mice. Blood samples were centrifuged at 10 000*g* for 15 minutes at 4°C to isolate the serum.[21] Serum concentrations of interleukin (IL)–1α, IL-1β, IL-2, IL-3, IL-4, IL-5, IL-6, IL-9, IL-10, IL-12(p40), IL-12(p70), IL-13, IL-17, Eotaxin, granulocyte colony-stimulating factor (CSF), granulocyte–macrophage–CSF, interferon (IFN)–γ, keratinocyte-derived chemokine (KC), monocyte chemotactic protein-1, macrophage inflammatory protein (MIP)–1α, MIP-1β, Regulated upon Activation, Normal T-cell Expressed, and Secreted, tumor necrosis factor-α, IL-15, fibroblast growth factor-basic, leukemia inhibitory factor, macrophage-CSF, human monokine induced by gamma interferon, MIP-2, platelet-derived growth factorβ, and vascular endothelial growth factor were measured using the Bio-Plex Pro assay (Bio-Rad). Serum soluble IL-2 receptor α (sIL-2Rα) concentrations were determined by ELISA (DuoSet ELISA Development System; R&D Systems). Serum aspartate aminotransferase (AST) and alanine aminotransferase (ALT) activities were determined using a commercially available kit (Transaminase CII test; Wako Pure Chemical Industries).

Histology and immunohistochemical staining

Mouse tissues were fixed with 4% formaldehyde (Mildform 10 N; Wako Pure Chemical Industries), dehydrated with an ethanol series, embedded in paraffin, sectioned (10-μm thick) and stained with hematoxylin and eosin. For tissue immunostaining, paraffin was removed from the sections using xylene following the standard method,[14] and sections were incubated with anti-CD3 or anti-CD45R (Santa Cruz Biotechnology) in phosphate-buffered saline without Ca^{2+} and Mg^{2+} (pH 7.4) but with 5% skim milk. Next, the sections were incubated with biotinylated anti-rat immunoglobulin (Ig)G (1:500), followed by incubation with horseradish peroxidase-conjugated avidin-biotin complex (Dako Corp), and the color reaction was developed using 3,3′-diaminobenzidine. Sections were observed under an optical microscope (Carl Zeiss).

Detection of immunoglobulin gene rearrangements by PCR

Genomic DNA was isolated from tumor tissues, and PCR was performed as described.[22] In brief, PCR reaction conditions were 98°C for 3 minutes; 30 cycles at 98°C for 30 seconds, 60°C for 30 seconds, 72°C for 1.5 minutes, and 72°C for 10 minutes. Mouse Vk genes were amplified using previously described primers.[23] Amplification of mouse Vj genes was performed using Vκcon (5′-GGCTGCAGSTTCAGTGGCAGTGGRTCWGGRAC-3′; R, purine; W, A or T) and Jκ5 (5′-TGCCACGTCAACTGATAATGAGCCCTCTC-3′) as described.[24]

Results

Establishment of transgenic mice with B lineage–restricted HCV gene expression

We defined the direct effect of HCV infection on B cells in vivo by crossing transgenic mice that had an integrated full-length HCV genome (Rz) under the conditional Cre/*lox*P expression system (Figure 1A upper schematic)[12,19,25] with mice that expressed the Cre enzyme under transcriptional control of the B lineage–restricted gene *CD19*[17] (RzCD19Cre; Figure 1A lower schematic). Expression of the HCV transgene in RzCD19Cre mice was confirmed by ELISA (Figure 1B); a substantial level of HCV core protein was detected in the spleen (370.9 ± 10.2 pg/mg total protein), but levels were lower in the liver (0.32 ± 0.03 pg/mg) and plasma (not detectable). RT-PCR analysis of peripheral blood lymphocytes (PBLs) from RzCD19Cre mice indicated the presence of HCV transcripts (Figure 1C). The weights of RzCD19Cre, Rz (with the full HCV genome transgene alone), CD19Cre (with the Cre gene knock-in at the CD19 gene locus) and WT mice were measured weekly for more than 600 days post birth; there were no significant differences between these groups (data not shown; the total number of transgenic and WT mice was approximately 200). The survival rate in each group was also measured for > 600 days (Figure 1D); survival in the female RzCD19Cre group was lower than that of the other groups.

The spontaneous development of B-cell lymphomas in the RzCD19Cre mouse

At 600 days post birth, mice (n = 140) were killed by bleeding under anesthesia, and tissues (spleen, lymph node, liver, and tumors) were excised and examined by hematoxylin and eosin staining (Figure 2A; supplemental Figure 1, available on the *Blood* Web site; see the Supplemental Materials link at the top of the online article). The incidence of B-cell lymphoma in RzCD19Cre mice was 25.0% (22.2% in males and 29.6% in females) and was significantly higher than the incidence in the HCV-negative groups (Table 1). This incidence is significantly higher than those of the other cell-type tumors developed spontaneously in all mouse groups (supplemental Table 1). Because nodular proliferation of CD45R-positive atypical lymphocytes was observed, lymphomas were diagnosed as typical diffuse B-cell non-Hodgkin lymphomas (Figure 2Aiv,vi-vii; supplemental Figure 1B,E,H,M). Mitotic cells were also positive for CD45R (Figure 2Avi arrowheads). CD3-positive T-lymphocytes were small and had a scattered distribution. Intrahepatic lymphomas had the same immunophenotypic characteristics as B-cell lymphomas (supplemental Figure 1K arrowheads, inset; 1L–N, ID No. 24-4, RzCD19Cre mouse); lymphoma tissues were markedly different compared with the control lymph node (Figure 2Ai,iii,v; ID No. 47-4, CD19Cre mouse) and liver (supplemental Figure 1J; ID No. 24-2, Rz mouse; tissues were from a littermate of the mice used to generate the data in supplemental Figure 1D-I,K-N). All samples were reviewed by at least 2 expert pathologists and classified according to World Health Organization classification.[26] Lymphomas were mostly CD45R positive and located in the mesenteric lymph nodes (Figure 2A; supplemental Figure 1), and some were identified as intrahepatic lymphomas (incidence, 4.2%; supplemental Figure 1K-N). HCV gene expression was detected in all B-cell lymphomas of RzCD19Cre mice (Figure 2B).

To examine the Ig gene configuration in the B-cell lymphomas of the RzCD19Cre mice, genomic DNA was isolated and analyzed by PCR. Ig gene rearrangements were identified in each case (Figure 2C). Genomic DNA isolated from the tumors of a germinal center–associated nuclear protein (GANP) transgenic mouse (GANP Tg#3) yielded a predominant Jk5 PCR product (Figure 2C, Vκ-Jκ); a predominant JH1 product and a minor JH2 product (supplemental Figure 2, DH-JH) were also identified, as previously reported,[22] indicating that the lymphoma cells proliferated from the transformation of an oligo B-cell clone. The B-cell lymphomas of

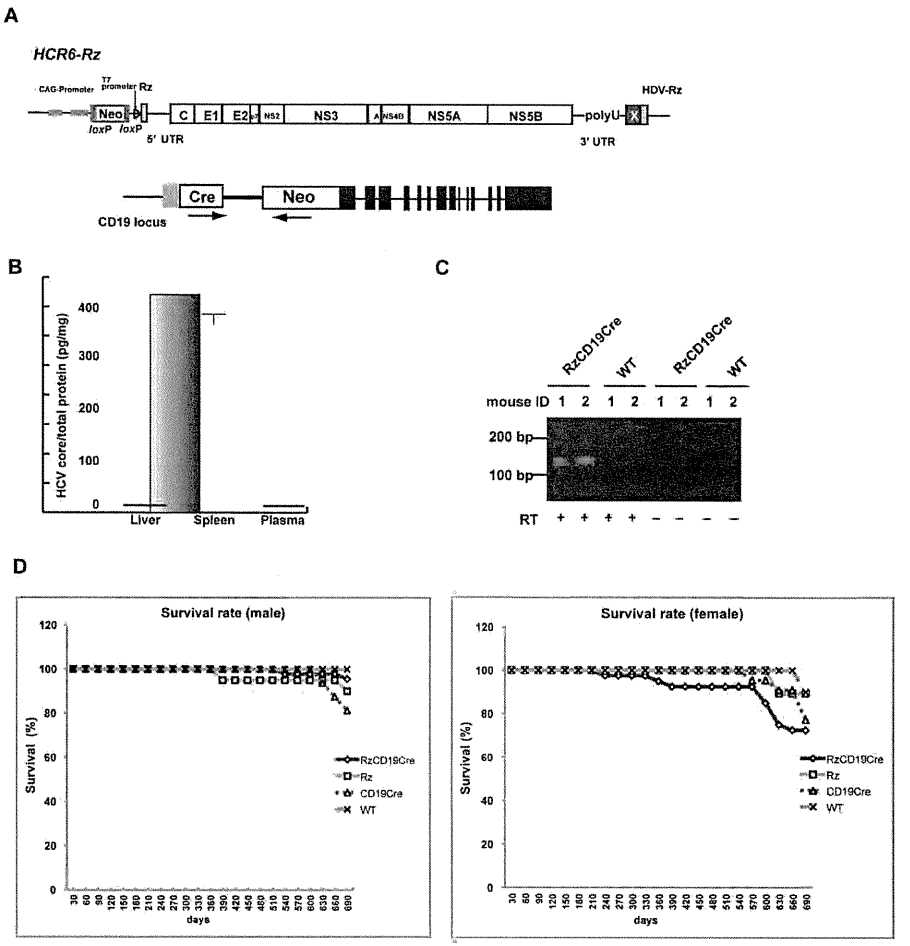

Figure 1. Establishment of RzCD19Cre mice. (A) Schematic diagram of the transgene structure comprising the complete HCV genome (*HCR6-Rz*). HCV genome expression was regulated by the Cre/*lox*P expression cassette (top diagram). The Cre transgene was located in the CD19 locus (bottom diagram). (B) Expression of HCV core protein in the liver, spleen, and plasma of RzCD19Cre mice was quantified by core ELISA. Data represent the mean ± SD (n = 3). (C) Detection of HCV RNA in PBLs by RT-PCR. Samples that included the RT reaction are indicated by +, and those that did not include the RT reaction are indicated by –. (D) Survival rates of male and female RzCD19Cre mice (males, n = 45; females, n = 40), Rz mice (males, n = 20; females, n = 19), CD19Cre mice (males, n = 16; females, n = 22), and WT mice (males, n = 5; females, n = 10).

8 RzCD19Cre mice (mouse ID Nos. 24-1, 54-1, 56-5, 69-5, 42-4, 43-4, 36-3 [data not shown] and 62-2 [data not shown]) yielded a Jκ-5 gene amplification product, and the lymphomas from 3 other mice had the alternative gene configurations Jκ-1 (mouse ID No. 31-4), Jκ-2 (mouse ID No. 24-4) and Jκ-3 (mouse ID No. 42-4; Figure 2C). PCR amplification products from the genes JH4 (mouse ID Nos. 24-1, 24-4, 54-1, 43-4, 56-5, 69-5, 62-2 [data not shown], 36-3 [data not shown]), JH1 (mouse ID Nos. 31-4, 42-4) and JH3 (mouse ID Nos. 31-4, 42-4, 56-5, 43-4, 36-3 [data not shown]) were also detected (supplemental Figure 2). The mutation frequencies in the Jκ-1, -3 and -5 genes were the same as the mutation frequency in the genomic V-region gene.[22] Few or no sequence differences in the variable region were identified among clones from which DNA was amplified. These results indicate the possibility that tumors judged as B-cell lymphomas based on pathology criteria were derived from the transformation of a single germinal center of B-cell origin.

To rule out the oncogenic effect caused by a transgenic integration into a specific genomic locus, we examined if HCV transgene inserted into another genomic site also causes B-cell lymphomas using another HCV transgenic mouse strain, MxCre/CN2-29 (supplemental Figure 3). Expression of the HCV CN2

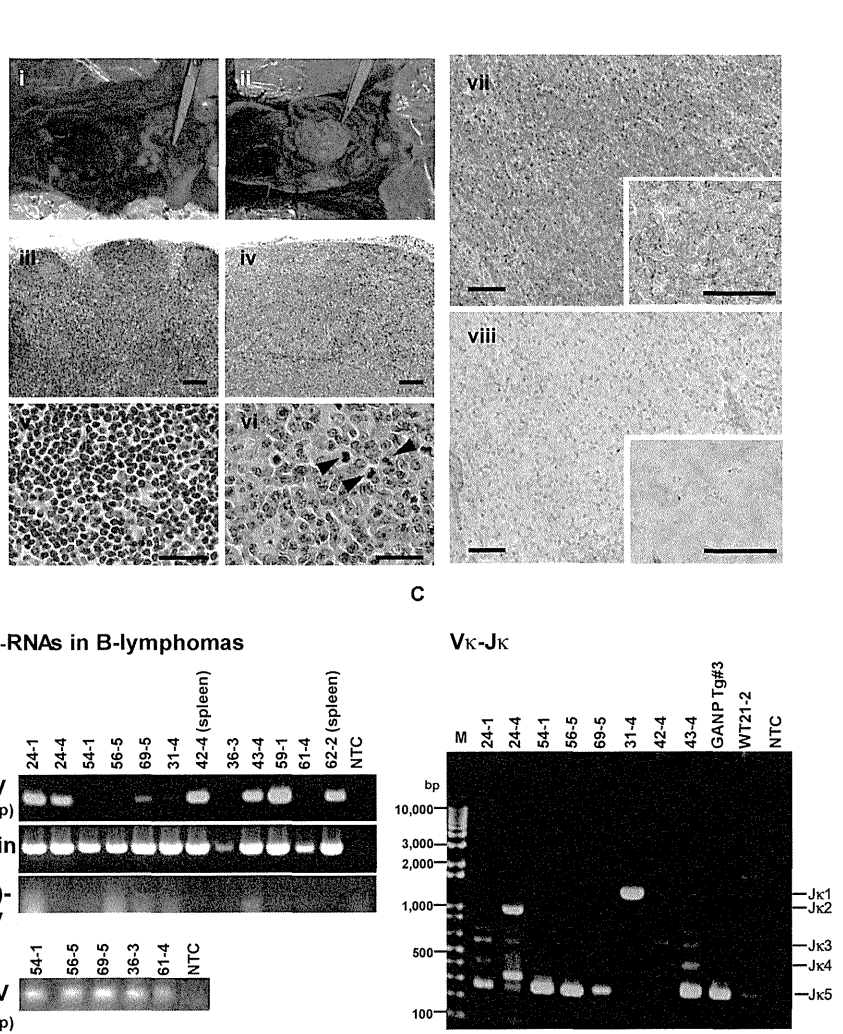

Figure 2. Histopathologic analysis of B-cell lymphomas in RzCD19Cre mouse tissues. (A) Histologic analysis of tissues from a normal mouse (i, iii, v; CD19Cre mouse, ID No. 47-4, male) and a B-cell lymphoma from a RzCD19Cre mouse (ii, iv, vi; ID No. 69-5, male). Paraformaldehyde-fixed and paraffin-embedded tumor tissues were stained with hematoxylin and eosin (iii-vi) or immunostained using anti-CD45R (vii; bottom right, inset) and anti-CD3 (viii; bottom right, inset). Also shown is a macroscopic view of the lymphoma from a mesenchymal lymph node (ii, indicated by forceps), which is not visible in the normal mouse (i). Mitotic cells are indicated with arrowheads (vi). Scale bars: 100 μm (iii-iv, vii-viii) and 20 μm (v-vi, insets in vii-viii). (B) Expression of HCV RNA in B-cell lymphomas from RzCD19Cre mice was examined by RT-PCR. The first round of PCR amplification yielded a 123-base pair fragment of HCV cDNA (upper panel), and a second round of PCR amplification yielded a 65-base pair fragment (lower panel). The β-actin mRNA was a control. As an additional control, the first and second rounds of amplification were performed using samples that had not been subjected to reverse transcription. NTC, no-template control. (C) Ig gene rearrangements in the tumors of RzCD19Cre mice. Genomic DNA isolated from B-cell lymphoma tissues of RzCD19Cre mice (ID Nos. 24-1, 24-4, 54-1, 56-5, 69-5, 31-4, 42-4, 43-4) and spleen tissues of a WT mouse (ID No. 21-2) was PCR amplified using primers specific for Vκ-Jκ genes. Amplification of controls was performed using genomic DNA isolated from a GANP transgenic mouse (GANP Tg#3) and in the absence of template DNA (no-template control, NTC). M, DNA ladder marker.

gene (nucleotides 294-3435)[12] was induced by the Mx promoter-driven cre recombinase with poly(I:C) induction[14] (supplemental Figure 3A). HCV core proteins were detected in both normal spleen (mouse ID Nos. 2, 3, 4) and intra-splenic B-cell lymphoma tissues

Table 1. Lymphoma incidence in HCV-expressing and control mice

HCV expression	Mouse genotype	No.	Incident B lymphoma, number (%)	Incident T lymphoma, number (%)
+	RzCD19Cre	72	18 (25.0)	3 (4.1)
−	Rz	34	1 (2.9)	1 (2.9)
−	CD19Cre	22	2 (9.1)	1 (4.5)
−	WT	12	1 (8.3)	1 (8.3)

(mouse ID Nos. 5, 6, 7) of MxCre/CN2-29 mice but not in spleens of the CN2-29 mouse (mouse ID No. 1, Figure 3B). After 12 months, the MxCre/CN2-29 mice developed B-cell lymphomas in the spleen at a high incidence (33.3%: 3/9), whereas the CN2-29 mice did not (0/13; supplemental Figure 3C), indicating that the development of B-cell lymphomas in HCV transgenic mice occurred similarly to RzCD19Cre mice. MxCre/CN2-29 mice also developed hepatocellular carcinomas (10%, 360 days, 17%, 480 days, 50%, 600 days after onset of HCV expression; Sekiguchi et al, submitted).

The results obtained in 2 HCV transgenic mouse strains indicate that the expression of the HCV gene or the proteins indeed induces the spontaneous development of B-cell lymphomas irrespective of the integrated site in the mouse genome.

The levels of cytokines and chemokines in B-cell lymphomas and other tumors and in tumor-free control mice

Abnormal induction of cytokine production occurs in HCV-associated non-Hodgkin lymphomas[27,28] and in patients with

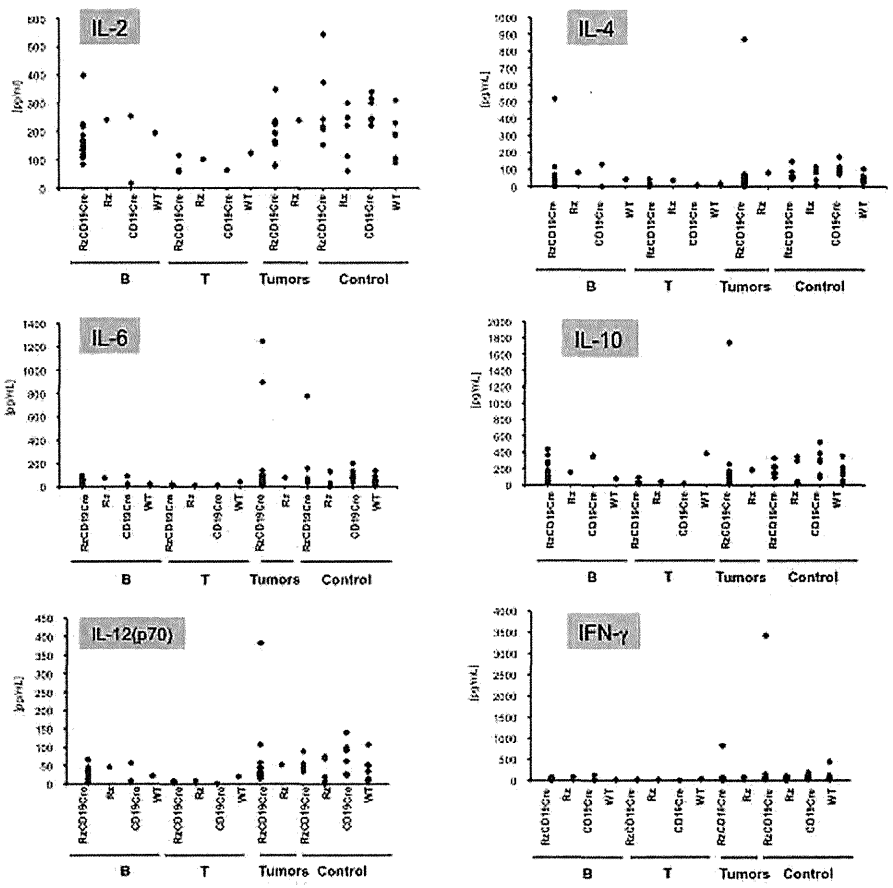

Figure 3. Analysis of serum cytokine levels using a multisuspension array system. The serum concentration levels of IL-2, IL-4, IL-6, IL-10, IL-12(p70), and IFN-γ were measured in RzCD19Cre mice with B-cell lymphomas (B), T-cell lymphomas (T), and other tumors (mammary tumor, sarcoma, and hepatocellular carcinoma) and in tumor-free RzCD19Cre, Rz, CD19Cr,e and WT mice.

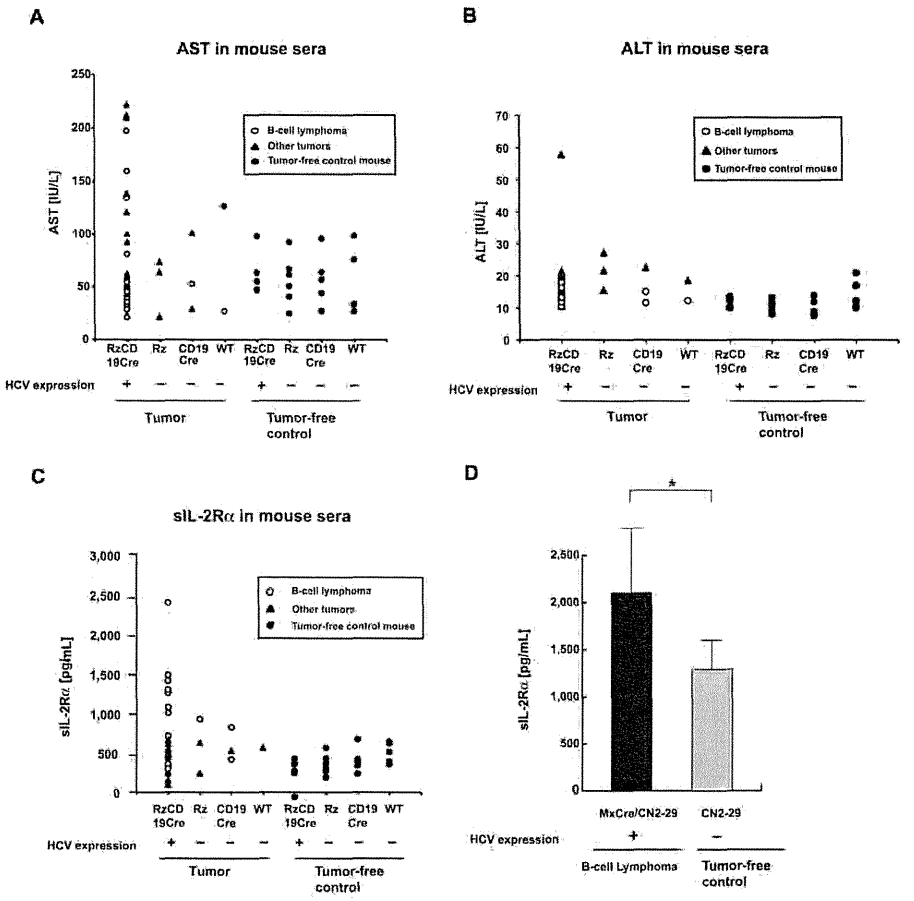

Figure 4. Serum titers of AST, ALT and soluble IL-2Rα in transgenic and control mice lacking or harboring B-cell lymphomas. (A-B) The AST (A) and ALT (B) assays were performed on serum samples from tumor-free control mice and the RzCD19Cre, Rz, CD19Cre and WT mice with or without B-cell lymphomas or other tumors. (C) ELISA analysis was performed to determine the sIL-2Rα concentration in serum samples from tumor-free control mice and the RzCD19Cre, Rz, CD19Cre, and WT mice with or without B-cell lymphomas or other tumors. (D) Concentration of soluble IL-2Rα in sera from transgenic (MxCre/CN2-29 or CN2-29) mice with or without B-cell lymphomas (* $P < .05$).

chronic hepatitis.[29,30] Therefore, we examined tumor cytokine and chemokine levels using a multisuspension array system. The levels of IL-2, IL-4, IL-6, IL-10, IL-12(p70), and IFN-γ (Figure 3), which may have a link with lymphoproliferation[14] or lymphoma[28,31] induced by HCV, and IL-1α, IL-1β, IL-3, IL-5, IL-9, IL-12(p40), IL-13, IL-17, Eotaxin, granulocyte-CSF, granulocyte–macrophage–CSF, KC, monocyte chemotactic protein-1, MIP-1α, MIP-1β, Regulated upon Activation, Normal T-cell Expressed, and Secreted, tumor necrosis factor-α, IL-15, fibroblast growth factor-basic, leukemia inhibitory factor, macrophage-CSF, human monokine induced by gamma interferon, MIP-2, platelet-derived growth factorβ and vascular endothelial growth factor (supplemental Figure 4) were measured in sera from mice with B-cell lymphomas, T-cell lymphomas, and other tumors and in sera from tumor-free RzCD19Cre, Rz, CD19Cre, and WT control mice. The levels of these cytokines and chemokines in sera from tumor-bearing RzCD19Cre mice with B-cell lymphomas were not significantly different from those of the control groups, and thus, changes in the expression of these cytokines and chemokines were not strictly correlated with the occurrence of B-cell lymphoma in RzCD19Cre mice.

The levels of amino transferases and sIL-2Rα in mice lacking or harboring B-cell lymphomas

We also examined the levels of AST and ALT in the RzCD19Cre, Rz, CD19Cre, and WT mice. There were no significant differences in the levels of AST and ALT in the sera of mice lacking or harboring B-cell lymphomas ($P > .05$; Figure 4A-B; AST:

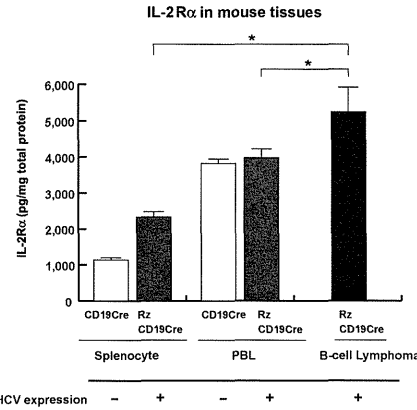

Figure 5. Levels of IL-2Rα in transgenic and control mice lacking or harboring B-cell lymphomas. The expression level of IL-2Rα in splenocytes and PBLs from CD19Cre and RzCD19Cre mice and in B-cell lymphomas from RzCD19Cre mice was measured by ELISA. IL-2Rα levels per total protein are indicated (picograms per milligram). Data from quadruplicate samples are shown as the mean ± SD (* $P < .05$).

RzCD19Cre mice with B-cell lymphomas, 72.2 ± 60.5 IU/L; normal controls, 55.2 ± 23.0 IU/L and ALT: RzCD19Cre mice with B-cell lymphomas, 14.2 ± 3.1 IU/L; normal controls, 11.5 ± 3.0 IU/L).

Finally, we examined the level of sIL-2Rα in the sera of the RzCD19Cre mice with B-cell lymphomas; sIL-2Rα is generated by proteolytic cleavage of IL-2Rα (CD25) residing on the surface of activated T and natural killer cells, monocytes, and certain tumor cells.[24,32] The average sIL-2Rα level in the RzCD19Cre mice with B-cell lymphomas (830.3 ± 533.0 pg/mL) was significantly higher than that in the tumor-free control groups, including the RzCD19Cre, Rz, CD19Cre and WT mice (499.9 ± 110.2 pg/mL; $P < .0057$; Figure 4C). The average sIL-2Rα levels in other tumor-containing groups (430.46 ± 141.15 pg/mL) were not significantly different from those in the tumor-free control groups ($P > .05$; Figure 4C). Moreover, all RzCD19Cre mice with a relatively high level of sIL-2Rα (> 1000 pg/mL) presented with B-cell lymphomas (Figure 4C).

We also examined the level of sIL-2Rα in MxCre/CN2-29 mice and observed a significant increase in sIL-2Rα in mice that expressed HCV and that had B-cell lymphomas compared with tumor-free control (CN2-29) mice (Figure 4D).

Expression of IL-2Rα in B-cell lymphomas of the RzCD19Cre mice

To examine whether sIL-2Rα was derived from lymphoma tissues, we quantified IL-2Rα concentrations in splenocytes, PBLs and B-cell lymphoma tissues (Figure 5). The concentration of IL-2Rα was significantly higher in splenocytes from RzCD19Cre mice compared with those from CD19Cre mice; the concentration was even higher in B-cell lymphoma tissues than in splenocytes from RzCD19Cre mice (Figure 5). These results strongly suggest that B-cell lymphomas directly contribute to the elevated serum concentrations of sIL-2Rα in RzCD19Cre mice.

Discussion

We have established HCV transgenic mice that have a high incidence of spontaneous B-cell lymphomas. In this animal model, the HCV transgene is expressed during the embryonic stage, and these RzCD19Cre mice are expected to be immunotolerant to the HCV transgene product. Thus, the results from this study reveal the potential for the HCV gene to induce B-cell lymphomas without inducing host immune responses against the HCV gene product. A retrospective study indicated that viral elimination reduced the incidence of malignant lymphoma in patients infected with HCV.[33] The results in our study may be consistent with this retrospective observation, indicating the significance of the direct effect of HCV infection on B-cell lymphoma development. Another HCV transgenic mouse strain (MxCre/CN2-29) showed the similarly high incidence of B-cell lymphoma, which strongly supported that development of B-cell lymphomas occurred by the expression of HCV transgene.

Recent findings have revealed the significance of B lymphocytes in HCV infection of liver-derived hepatoma cells.[34] In 4.2% of the RzCD19Cre mice, CD45R-positive intrahepatic lymphomas were identified, and infiltration of B cells into the hepatocytes was frequently observed (data not shown). These phenomena suggest that HCV could modify the in vivo tropism of B cells. The RzCD19Cre mouse is a powerful model system to address these mechanisms in vivo.

As a circulating membrane receptor, sIL-2Rα is localized in lymphoid cells and some other types of cancer cells and is highly expressed in several cancers[35-40] and autoimmune diseases.[41] Recent findings indicate a link between sIL-2Rα levels and hepatocellular carcinoma in Egyptian patients.[42] Appearing on the surface of leukemic cells derived from B and pre-B lymphocytes and other leukemic cells, IL-2Rα is one of the subunits of the IL-2 receptor, which is composed of an α chain (CD25), a β chain (CD122), and a γ chain (CD132).[43] IL-2R ectodomains are thought to be proteolytically cleaved from the cell surface[34,44,45] instead of produced as a result of posttranscriptional splicing.[24] In RzCD19Cre splenocytes, the level of IL-2Rα was higher than that in splenocytes from CD19Cre mice; however, serum concentrations of sIL-2Rα in RzCD19Cre mice without B-cell lymphomas did not show significant differences compared with other control groups (Rz, CD19Cre, and WT). These results indicate the possibility that HCV may increase IL-2Rα expression on B-cells; proteolytic cleavage of IL-2Rα was increased after B-cell lymphoma development in the RzCD19Cre mouse. The detailed mechanism that induces IL-2Rα as a result of HCV expression is still unclear at present, but we have found previously that the HCV core protein induces IL-10 expression in mouse splenocytes.[14] IL-10 up-regulates the expression of IL-2Rα (Tac/CD25) on normal and leukemic B lymphocytes,[46] and therefore, through IL-10, the HCV core protein might induce IL-2Rα in B cells of the RzCD19Cre mouse.

In conclusion, this study established an animal model that will likely provide critical information for the elucidation of molecular mechanism(s) underlying the spontaneous development of B-cell non-Hodgkin lymphoma after HCV infection. This knowledge should lead to therapeutic strategies to prevent the onset and/or progression of B-cell lymphomas.

Acknowledgments

We thank Dr T. Ito for assistance with pathology characterization and Dr T. Munakata for valuable comments.

This work was supported by grants from the Ministry of Health and Welfare of Japan and the Cooperative Research Project on Clinical and Epidemiologic Studies of Emerging and Re-emerging Infectious Diseases.

Authorship

Contribution: K.T.-K. conceived of the project; K.K., M.K., and K.T.-K. designed the studies; Y.K., S.S., M. Saito, K.T., M. Satoh, M.T., and K.T.-K. performed experiments and analyses; N.S. and Y.H. provided scientific advice; and K.T.-K. wrote the manuscript.

Conflict-of-interest disclosure: The authors declare no competing financial interests.

Correspondence: Kyoko Tsukiyama-Kohara, Department of Experimental Phylaxiology, Faculty of Life Sciences, Kumamoto University, Kumamoto 860-8556, Japan; e-mail: kkohara@kumamoto-u.ac.jp.

References

1. Ferri C, Monti M, La Civita L, et al. Infection of peripheral blood mononuclear cells by hepatitis C virus in mixed cryoglobulinemia. *Blood.* 1993; 82(12):3701-3704.
2. Saito I, Miyamura T, Ohbayashi A, et al. Hepatitis C virus infection is associated with the development of hepatocellular carcinoma. *Proc Natl Acad Sci U S A.* 1990;87(17):6547-6549.
3. Simonetti RG, Camma C, Fiorello F, et al. Hepatitis C virus infection as a risk factor for hepatocellular carcinoma in patients with cirrhosis. A case-control study. *Ann Intern Med.* 1992;116(2):97-102.
4. Silvestri F, Pipan C, Barillari G, et al. Prevalence of hepatitis C virus infection in patients with lymphoproliferative disorders. *Blood.* 1996;87(10): 4296-4301.
5. Ascoli V, Lo Coco F, Artini M, Levrero M, Martelli M, Negro F. Extranodal lymphomas associated with hepatitis C virus infection. *Am J Clin Pathol.* 1998;109(5):600-609.
6. Mele A, Pulsoni A, Bianco E, et al. Hepatitis C virus and B-cell non-Hodgkin lymphomas: an Italian multicenter case-control study. *Blood.* 2003; 102(3):996-999.
7. Dammacco F, Sansonno D, Piccoli C, Racanelli V, D'Amore FP, Lauletta G. The lymphoid system in hepatitis C virus infection: autoimmunity, mixed cryoglobulinemia, and overt B-cell malignancy. *Semin Liver Dis.* 2000;20(2):143-157.
8. Gisbert JP, Garcia-Buey L, Pajares JM, Moreno-Otero R. Prevalence of hepatitis C virus infection in B-cell non-Hodgkin's lymphoma: systematic review and meta-analysis. *Gastroenterology.* 2003;125(6):1723-1732.
9. Negri E, Little D, Boiocchi M, La Vecchia C, Franceschi S. B-cell non-Hodgkin's lymphoma and hepatitis C virus infection: a systematic review. *Int J Cancer.* 2004;111(1):1-8.
10. Pileri P, Uematsu Y, Campagnoli S, et al. Binding of hepatitis C virus to CD81. *Science.* 1998; 282(5390):938-941.
11. Rosa D, Saletti G, De Gregorio E, et al. Activation of naive B lymphocytes via CD81, a pathogenetic mechanism for hepatitis C virus-associated B lymphocyte disorders. *Proc Natl Acad Sci U S A.* 2005;102(51):18544-18549.
12. Wakita T, Taya C, Katsume A, et al. Efficient conditional transgene expression in hepatitis C virus cDNA transgenic mice mediated by the Cre/loxP system. *J Biol Chem.* 1998;273(15):9001-9006.
13. Machida K, Tsukiyama-Kohara K, Seike E, et al. Inhibition of cytochrome c release in Fas-mediated signaling pathway in transgenic mice induced to express hepatitis C viral proteins. *J Biol Chem.* 2001;276(15):12140-12146.
14. Machida K, Tsukiyama-Kohara K, Sekiguch S, et al. Hepatitis C virus and disrupted interferon signaling promote lymphoproliferation via type II CD95 and interleukins. *Gastroenterology.* 2009; 137(1):285-296,296 e281-211.
15. Lerat H, Rumin S, Habersetzer F, et al. In vivo tropism of hepatitis C virus genomic sequences in hematopoietic cells: influence of viral load, viral genotype, and cell phenotype. *Blood.* 1998; 91(10):3841-3849.
16. Karavattathayyil SJ, Kalkeri G, Liu HJ, et al. Detection of hepatitis C virus RNA sequences in B-cell non-Hodgkin lymphoma. *Am J Clin Pathol.* 2000;113(3):391-398.
17. Rickert RC, Roes J, Rajewsky K. B lymphocyte-specific, Cre-mediated mutagenesis in mice. *Nucleic Acids Res.* 1997;25(6):1317-1318.
18. Tanaka T, Lau JY, Mizokami M, et al. Simple fluorescent enzyme immunoassay for detection and quantification of hepatitis C viremia. *J Hepatol.* 1995;23(6):742-745.
19. Tsukiyama-Kohara K, Tone S, Maruyama I, et al. Activation of the CKI-CDK-Rb-E2F pathway in full genome hepatitis C virus-expressing cells. *J Biol Chem.* 2004;279(15):14531-14541.
20. Nishimura T, Kohara M, Izumi K, et al. Hepatitis C virus impairs p53 via persistent overexpression of 3beta-hydroxysterol Delta24-reductase. *J Biol Chem.* 2009;284(52):36442-36452.
21. Tsukiyama-Kohara K, Poulin F, Kohara M, et al. Adipose tissue reduction in mice lacking the translational inhibitor 4E-BP1. *Nat Med.* 2001; 7(10):1128-1132.
22. Fujimura S, Xing Y, Takeya M, et al. Increased expression of germinal center-associated nuclear protein RNA-primase is associated with lymphomagenesis. *Cancer Res.* 2005;65(13):5925-5934.
23. Miyazaki T, Kato I, Takeshita S, Karasuyama H, Kudo A. Lambda5 is required for rearrangement of the Ig kappa light chain gene in pro-B cell lines. *Int Immunol.* 1999;11(8):1195-1202.
24. Rubin LA, Galli F, Greene WC, Nelson DL, Jay G. The molecular basis for the generation of the human soluble interleukin 2 receptor. *Cytokine.* 1990;2(5):330-336.
25. Tsukiyama-Kohara K, Iizuka N, Kohara M, Nomoto A. Internal ribosome entry site within hepatitis C virus RNA. *J Virol.* 1992;66(3):1476-1483.
26. Jaffe ES, Harris NL, Stein H, Isaacson PG. Classification of lymphoid neoplasms: the microscope as a tool for disease discovery. *Blood.* 2008; 112(12):4384-4399.
27. el-Din HM, Attia MA, Hamza MR, Khaled HM, Thoraya MA, Eisa SA. Hepatitis C Virus and related changes in immunologic parameters in non Hodgkin's lymphoma patients. *Egypt J Immunol.* 2004;11(1):55-64.
28. Feldmann G, Nischalke HD, Nattermann J, et al. Induction of interleukin-6 by hepatitis C virus core protein in hepatitis C-associated mixed cryoglobulinemia and B-cell non-Hodgkin's lymphoma. *Clin Cancer Res.* 2006;12(15):4491-4498.
29. Mizuochi T, Ito M, Takai K, Yamaguchi K. Differential susceptibility of peripheral blood CD5+ and CD5− B cells to apoptosis in chronic hepatitis C patients. *Biochem Biophys Res Commun.* 2009; 389(3):512-515.
30. Bansal AS, Bruce J, Hogan PG, Prichard P, Powell EE. Serum soluble CD23 but not IL8, IL10, GM-CSF, or IFN-gamma is elevated in patients with hepatitis C infection. *Clin Immunol Immunopathol.* 1997;84(2):139-144.
31. Barrett L, Gallant M, Howley C, et al. Enhanced IL-10 production in response to hepatitis C virus proteins by peripheral blood mononuclear cells from human immunodeficiency virus-monoinfected individuals. *BMC Immunol.* 2008;9:28.
32. Rubin LA, Kurman CC, Fritz ME, et al. Soluble interleukin 2 receptors are released from activated human lymphoid cells in vitro. *J Immunol.* 1985;135(5):3172-3177.
33. Kawamura Y, Ikeda K, Arase Y, et al. Viral elimination reduces incidence of malignant lymphoma in patients with hepatitis C. *Am J Med.* 2007; 120(12):1034-1041.
34. Stamataki Z, Shannon-Lowe C, Shaw J, et al. Hepatitis C virus association with peripheral blood B lymphocytes potentiates viral infection of liver-derived hepatoma cells. *Blood.* 2009;113(3): 585-593.
35. Wasik MA, Sioutos N, Tuttle M, Butmarc JR, Kaplan WD, Kadin ME. Constitutive secretion of soluble interleukin-2 receptor by human T cell lymphoma xenografted into SCID mice. Correlation of tumor volume with concentration of tumor-derived soluble interleukin-2 receptor in body fluids of the host mice. *Am J Pathol.* 1994;144(5): 1089-1097.
36. Tsai MH, Chiou SH, Chow KC. Effect of platelet activating factor and butyrate on the expression of interleukin-2 receptor alpha in nasopharyngeal carcinoma cells. *Int J Oncol.* 2001;19(5):1049-1055.
37. Yano T, Yoshino I, Yokoyama H, et al. The clinical significance of serum soluble interleukin-2 receptors in lung cancer. *Lung Cancer.* 1996;15(1):79-84.
38. Tesarova P, Kvasnicka J, Umlaufova A, Homolkova H, Jirsa M, Tesar V. Soluble TNF and IL-2 receptors in patients with breast cancer. *Med Sci Monit.* 2000;6(4):661-667.
39. Maccio A, Lai P, Santona MC, Pagliara L, Melis GB, Mantovani G. High serum levels of soluble IL-2 receptor, cytokines, and C reactive protein correlate with impairment of T cell response in patients with advanced epithelial ovarian cancer. *Gynecol Oncol.* 1998;69(3):248-252.
40. Matsumoto T, Furukawa A, Sumiyoshi Y, Akiyama KY, Kanayama HO, Kagawa S. Serum levels of soluble interleukin-2 receptor in renal cell carcinoma. *Urology.* 1998;51(1):145-149.
41. Pountain G, Hazleman B, Cawston TE. Circulating levels of IL-1beta, IL-6 and soluble IL-2 receptor in polymyalgia rheumatica and giant cell arteritis and rheumatoid arthritis. *Br J Rheumatol.* 1998;37(7):797-798.
42. Zekri AR, Alam El-Din HM, Bahnassy AA, et al. Serum levels of soluble Fas, soluble tumor necrosis factor-receptor II, interleukin-2 receptor and interleukin-8 as early predictors of hepatocellular carcinoma in Egyptian patients with hepatitis C virus genotype-4. *Comp Hepatol.* 2010:9(1):1.
43. Sheibani K, Winberg CD, van de Velde S, Blayney DW, Rappaport H. Distribution of lymphocytes with interleukin-2 receptors (TAC antigens) in reactive lymphoproliferative processes, Hodgkin's disease, and non-Hodgkin's lymphomas. An immunohistologic study of 300 cases. *Am J Pathol.* 1987;127(1):27-37.
44. Robb RJ, Rusk CM. High and low affinity receptors for interleukin 2: implications of pronase, phorbol ester, and cell membrane studies upon the basis for differential ligand affinities. *J Immunol.* 1986;137(1):142-149.
45. Sheu BC, Hsu SM, Ho HN, Lien HC, Huang SC, Lin RH. A novel role of metalloproteinase in cancer-mediated immunosuppression. *Cancer Res.* 2001;61(1):237-242.
46. Fluckiger AC, Garrone P, Durand I, Galizzi JP, Banchereau J. Interleukin 10 (IL-10) up-regulates functional high affinity IL-2 receptors on normal and leukemic B lymphocytes. *J Exp Med.* 1993; 178(5):1473-1481.

Comparative Immunology, Microbiology and Infectious Diseases 33 (2010) e81–e88

Contents lists available at ScienceDirect

Comparative Immunology, Microbiology and Infectious Diseases

journal homepage: www.elsevier.com/locate/cimid

Evaluation of a recombinant measles virus expressing hepatitis C virus envelope proteins by infection of human PBL-NOD/Scid/Jak3null mouse

Masaaki Satoh[a], Makoto Saito[a], Kohsuke Tanaka[a], Sumako Iwanaga[b], Salem Nagla Elwy Salem Ali[a,d], Takahiro Seki[e,1], Seiji Okada[b], Michinori Kohara[c], Shinji Harada[d], Chieko Kai[e], Kyoko Tsukiyama-Kohara[a,*]

[a] *Department of Experimental Phylaxiology, Faculty of Life Sciences, Kumamoto University, 1-1-1 Honjo, Kumamoto-city, Kumamoto 860-8556, Japan*
[b] *Division of Hematopoiesis, Center for AIDS Research, Kumamoto University, Japan*
[c] *Department of Microbiology and Cell Biology, Tokyo Metropolitan Institute of Medical Science, Japan*
[d] *Department of Medical Virology, Faculty of Life Sciences, Kumamoto University, Japan*
[e] *Laboratory of Animal Research Center, Institute of Medical Science, University of Tokyo, Japan*

ARTICLE INFO

Article history:
Received 27 January 2010
Accepted 21 February 2010

Keywords:
MV
HCV
E1
E2
Human PBL
NOD/Scid/Jak3null mouse

ABSTRACT

In this study, we infected NOD/Scid/Jak3null mice engrafted human peripheral blood leukocytes (hu-PBL-NOJ) with measles virus Edmonston B strain (MV-Edm) expressing hepatitis C virus (HCV) envelope proteins (rMV-E1E2) to evaluate the immunogenicity as a vaccine candidate. Although human leukocytes could be isolated from the spleen of mock-infected mice during the 2-weeks experiment, the proportion of engrafted human leukocytes in mice infected with MV (10^3–10^5 pfu) or rMV-E1E2 (10^4 pfu) was decreased. Viral infection of the splenocytes was confirmed by the development of cytopathic effects (CPEs) in co-cultures of splenocytes and B95a cells and verified using RT-PCR. Finally, human antibodies against MV were more frequently observed than E2-specific antibodies in serum from mice infected with a low dose of virus (MV, 10^0–10^1 pfu, and rMV-E1E2, 10^1–10^2 pfu). These results showed the possibility of hu-PBL-NOJ mice for the evaluation of the immunogenicity of viral proteins.

1. Introduction

Hepatitis C virus (HCV) is a member of the *Flaviviridae* family and is the causative agent of both chronic hepatitis and hepatocellular carcinoma (HCC) [1–3]. 170 million people are infected with HCV worldwide [4,5]. Despite prevention efforts and advanced treatment strategies, including combined PEGylated alpha interferron (PEGIFN-α) and ribavirin therapy [6,7], the clinical efficacy of this treatment is limited [8,9]. Alternative novel antiviral agents that have been shown to elicit effective responses in chronically infected patients, such as inhibitors of viral protease, helicase, and polymerase, are currently being developed but are expensive [10]. Therefore, the development of an effective vaccine that either induces the production of high-titer, long-lasting, and cross-reactive neutralising antibodies or induces a cellular immune response is important.

Immunological approaches to control HCV infection have proven to be ineffective, in part because HCV adapts to escape from the host immune system [11]. Furthermore, a high percentage of immunocompetent individuals

* Corresponding author. Tel.: +81 96 373 5560; fax: +81 96 373 55620.
E-mail address: kkohara@kumamoto-u.ac.jp (K. Tsukiyama-Kohara).

[1] Present address: Virology, Shionogi Research Laboratories, Shionogi & Co Ltd, Osaka, Japan.

0147-9571/$ – see front matter © 2010 Elsevier Ltd. All rights reserved.
doi:10.1016/j.cimid.2010.02.006

are infected by HCV despite their ability to mount an active immune response [12]. A preventive HCV vaccine is required to protect unexposed individuals from HCV infection. This vaccine will most likely need to target the viral envelope glycoprotein, E1 and E2, and must also be bivalent, safe, and provide long-lasting protective immunity. To address this challenge, we evaluated the immunogenicity of a live-attenuated recombinant vector derived from the pediatric measles virus (MV) that expresses HCV antigens. The MV vaccine is a well-known, live-attenuated vaccine and has proven to be one of the safest, most stable, and effective human vaccines [13]. This vaccine is produced on a large scale in many countries and used at low cost through the Extended Program on Immunisation of the WHO [14,15]. While this vaccine has been shown to induce life-long immunity with a single dose, boosting is effective. Efforts to develop vaccines using recombinant MV expressing different proteins derived from dengue virus [16,17], human immunodeficiency virus (HIV) [18–21], Human papilloma virus (HPV) [22], Severe acute respiratory syndrome (SARS) [23], or West Nile virus (WNV) [24] have been described. We constructed a recombinant MV expressing the E1 and E2 envelope glycoproteins of HCV (rMV-E1E2) [25] and demonstrated that this virus could infect B95a cells and express HCV E1.

HCV research has long been hampered by the lack of an animal model that reproduces HCV infection in humans. The model in which severe combined immunodeficient (SCID) mice are transplanted with human peripheral blood leukocyte (PBL) is a well-established system to study human immunity (hu-PBL-SCID). This mouse develops all human lymphoid cell lineages that repopulate the animal's lymphoid organs. Our group previously generated the non-obese diabetic (NOD)/SCID/Janus kinase 3 (Jak3) knockout (NOJ) mouse model and then established a human hemolymphoid system in this mouse [26,27]. In this study, we infect human PBL-transplanted NOJ mice with MV and rMV-E1E2 and then characterise the humoral immune responses elicited by the transplanted human cells, in order to evaluate rMV-E1E2 as a vaccine candidate.

2. Materials and methods

2.1. Cells

B95a cells, a marmoset B cell line [28], were used for viral titration and rescue, and were maintained in RPMI 1640 medium supplemented with 10% heat-inactivated foetal calf serum (FCS).

2.2. Plasmid construction and viral rescue

The cDNAs encoding HCV E1 and E2 were obtained from the plasmid HCR6CNS2 [29]. We used replication-competent MV-based vectors (pMV; Edmonston B strain of MV) [25]. The E1 and E2 cDNAs were cloned into the *Fse* I site of pMV and the resulting clone, pMV-E1E2, was used to rescue the infectious recombinant MV expressing the HCV envelope glycoproteins (rMV-E1E2), as reported previously [30].

2.3. Generation of humanised mice

Mice were reconstituted as described previously [26,27]. The NOD/SCID/JAK3^{null} strain was established by backcrossing JAK3^{null} and the NOD Cg-Prkdc^{Scid} strains for ten generations. All animal experiments were performed according to the guidelines of Institutional Animal Committee or Ethics Committee of Kumamoto University.

2.4. Preparation of human blood leukocytes and transplantation

Peripheral blood leukocytes were isolated from blood donors using Ficoll–Hypaque density gradient centrifugation. A total of 5×10^6 cells were transplanted into the spleen of irradiated (2 Gy) 4-week-old mice.

2.5. MV and MV-E1E2 infection

We injected 10^0–10^5 pfu of MV or 10^0–10^2 or 10^4 pfu of MV-E1E2 intraperitoneally for MV and MV-E1E2 infection, respectively. As a negative control, a group of mice was injected with RPMI 1640. Mice were monitored for 2 weeks and then euthanised. The spleens and peripheral blood were collected for analysis.

2.6. Flow cytometry

Isolated splenocytes were stained with APC-Cy7-conjugated anti-mouse CD45 (BD Pharmingen) to detect the murine leukocytes and either APC- or pacific blue-conjugated anti-human CD45 (DAKO) to detect human leukocytes. All data were analysed using FlowJo (Tree Star).

2.7. Confirmation of viral infection

The viral infection of the human leukocytes was confirmed using co-culture with B95a cells followed by RT-PCR. Suspensions of isolated splenocytes were co-cultured with B95a cells and the formation of cytopathic effects (CPEs) was monitored for 2 weeks. Additionally, RNA was isolated from the supernatant of the co-cultures using ISOGEN-LS (Nippon gene) according to manufacturer's instructions. MV RNA was detected using reverse transcript-PCR (RT-PCR) with the sense primer, 5′-ACTCGGTATCACTGCCGAGGATGCAAGGC-3′ (1256–1284) and anti-sense primer 5′-CAGCGTCGTCATCGCTCTCTCC-3′ (2077–2056) or 5′-atggcagaagagcaggcacg-3′ (1807–1826). HCV E1 or E2 was amplified using E1-S-1051 5′-ccgttgctgggtggcactta-3′ and E1-AS-1314 5′-atcatcatgtcccaagccat-3′ or E2-S-1600 5′-ctggcacatcaacaggactg-3′ and E2-AS-1960 5′-aaggagcagcacgtctgtct-3′.

2.8. ELISA

Anti-MV antibody titers were determined by using an ELISA assay. 96-well plates were coated with a 25 μg/ml solution of MV-infected B95a lysate or recombinant E2-expressing baculovirus-infected Sf9 lysate as antigen, respectively. The plates were consecutively incubated with

Author's personal copy

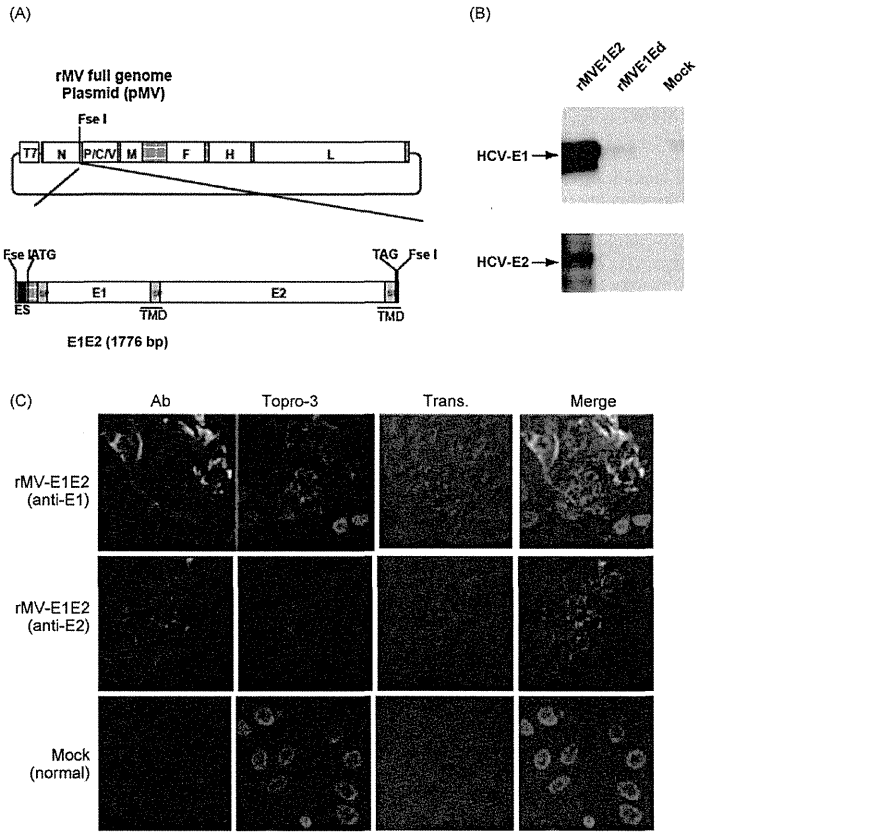

Fig. 1. Construction of the recombinant MV vectors. (A) The rMV full genome vector derived from the MV-Ed strain is illustrated in the upper panel and is labelled with letters as follows: N, nucleocapsid; P, phosphoprotein; M, matrix; F, fusion; H, hemagglutinin; and L, large. T7 indicates the T7 RNA polymerase promoter. The cDNA encoding the HCV envelope glycoproteins (E1 and E2) containing the signal peptide sequence (SP) and the transmembrane domain (TMD, underlined) regions, the N gene end signal (E), the P gene start signal (S), and the intercistronic region of the H protein genes at the 5′ end, which was flanked by Fse I sites at both ends, was introduced into the unique Fse I site in between the N and P genes in the pMV vector. The resulting plasmid was designated pMV-E1E2. (B) The HCV E1 and E2 proteins were detected in rMV-E1E2-, rMV-Ed- and mock-infected B95a cells by western blot with MoAb 384 and 544 (arrows). (C) rMV-E1E2-infected B95a cells were stained with MoAb 299 (anti-E1) or MoAb 187 (anti-E2) and analysed by immunofluorescence. Nuclei were stained with Topro-3 and the bright field and merged images are indicated (400×).

sera (1:100) recovered from hu-PBL-NOJ mice, peroxidase-conjugated rabbit-human IgG (DAKO), and TMB Peroxidase EIA Substrate Kit (Bio-Rad) at 37 °C for 1 h. Optimal density values were measured at 450 nm.

An anti-MV-NP antibody (Millipore, MA, USA) and normal mouse serum (NMS) were used as positive control and negative control respectively.

2.9. Western blot analysis

Total protein extracts from E2-expressing baculovirus-infected Sf9 lysate were separated by SDS-PAGE. The primary antibodies used for Western blots were as follows: sera from mice (1:100) and anti-E2 monoclonal antibody (1:5000). Peroxidase-conjugated secondary antibodies were added and incubated with the mixture for 1 h at room temperature.

3. Results

3.1. Construction of recombinant measles virus expressing E1 and E2

The HCV genes corresponding to the envelope proteins E1 and E2 were sub-cloned in between the N and P genes of the MV vector (Fig. 1A). The HCV E1 and E2 genes included

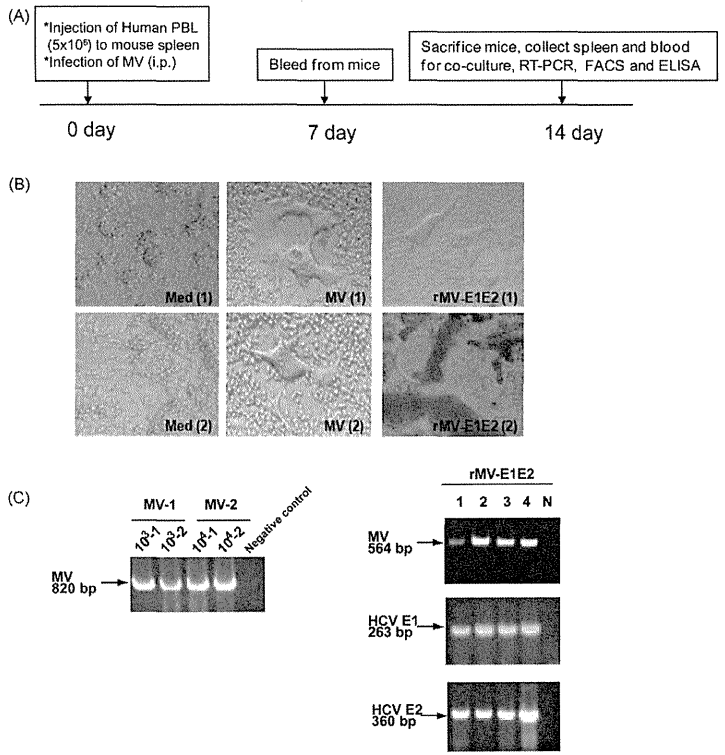

Fig. 2. Infection of hu-PBL-NOD/Scid mice with rMV and rMV-E1E2. (A) Course of infection of hu-PBL-NOD/SCID mice with MV and rMV-E1E2. (B) CPE formation in co-cultures of splenocytes isolated from MV- (MV1, 2), rMV-E1E2-, or mock-infected hu-PBL-NOD/SCID and B95a cells (40× magnification). (C) Detection of viral RNA by RT-PCR. Detection of MV in MV-1- or 2-infected mouse splenocyte co-cultures (820 bp) and rMV-E1E2-infected splenocyte co-cultures (564 bp), and HCV E1 (263 bp) and E2 (360 bp) in rMV-E1E2 (10^4 pfu)-infected splenocyte co-cultures (arrows).

the putative signal peptide sequences at the N terminus and the transmembrane domain at the C terminus [31]. The plasmid vector pMV-E1E2 was introduced with supporting plasmids into 293T cells to rescue the recombinant viruses. The expression of the E1 and E2 proteins by rMV-E1E2 was examined by Western blot (Fig. 1B) and immunofluorescence (Fig. 1C).

3.2. Infection of hu-PBL-NOJ mice with MV and rMV-E1E2

All hu-PBL-NOJ mouse infections were observed for 14 days (Fig. 2A). Infections with MV and rMV-E1E2 were confirmed by first co-culturing the human leukocytes isolated from the spleens of infected mice with B95a cells and then verifying the presence of virus by RT-PCR. In all the MV (10^3–10^4 pfu) or rMV-E1E2 (10^4 pfu)-infected hu-PBL-NOJ mice, CPEs were observed in co-cultures with splenocytes (Table 1; Fig. 2B). The results of the co-culture assays are in agreement with results that were obtained by RT-PCR; positive bands were observed in the mice infected with 10^3–10^4 pfu of MV and 10^4 pfu of rMV-E1E2 (Fig. 2C). These results demonstrate that the rescued MV and rMV-E1E2 are able to infect transplanted human PBL.

Table 1
Summary of MV and MV-E1E2 infection of hu-PBL-NOJ mice.

Virus	Amount of virus (PFU)	No. tested	CPE	RT-PCR
Mock	Medium	7	0/7	0/7
MV	10^0	3	0/3	0/3
	10^1	3	0/3	0/3
	10^2	3	0/3	0/3
	10^3	2	2/2	2/2
	10^4	2	2/2	2/2
MV-E1E2	10^0	3	0/3	0/3
	10^1	3	0/3	0/3
	10^2	3	0/3	1/3
	10^4	4	4/4	4/4

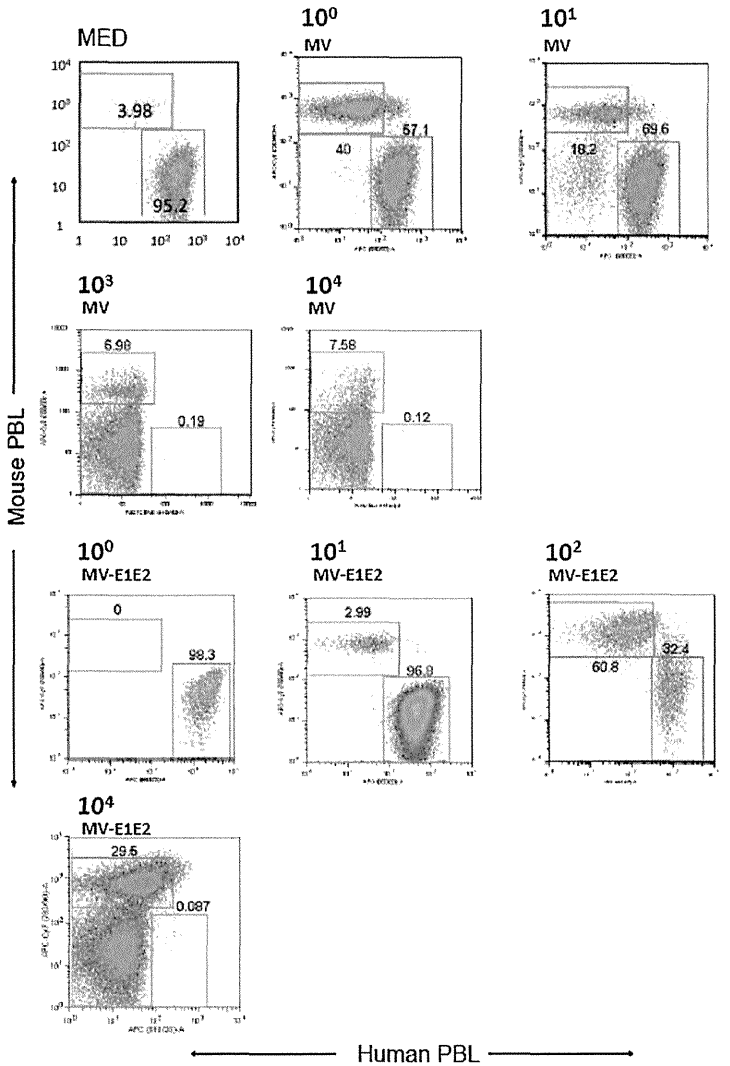

Fig. 3. Flow cytometric analysis of splenocytes isolated from hu-PBL-NOJ mice inoculated with medium, MV-Ed (10^0–10^4 pfu), or rMV-E1E2 (10^0–10^2 or 10^4 pfu). Splenocytes, consisting of both human and murine cells, were stained with antibodies against human or mouse CD45. Representative flow cytometric profiles of each group of infected mice are shown. The percentages of mouse and human leukocytes are shown.

3.3. Proportion of engrafted human leukocytes in MV- and rMV-E1E2- infected hu-PBL-NOJ mice

We also examined the splenocytes of infected mice simultaneously, using flow cytometry to determine the proportion of human cells in the spleen (Fig. 3, Table 2). In the MV-infected hu-PBL-NOJ mice, a population of human leukocytes was observed in the mice that were infected with 10^0–10^1 pfu, whereas few human leukocytes were observed in mice infected with 10^2–10^4 pfu. In contrast, in the rMV-E1E2-infected mice, a population of human leukocytes was detected in mice that were inoculated with 10^0–10^2 pfu. The ratio of human leukocytes settlement in both groups of mice was inversely correlated

Table 2
Proportion of human peripheral leukocytes in the spleen of MV-, rMV-E1E2, or mock-infected hu-PBL-NOJ mice.

Virus	Amount of virus (PFU)	No. tested	huPBL settlement (average ± S.D.%)
Mock	Medium	6	90.9 ± 13.1
MV	10^0	3	92.7 ± 11.2
	10^1	3	58.4 ± 50.6
	10^2	3	55.1 ± 49.9
	10^3	4	4.9 ± 6
	10^4	2	1.7
MV-E1E2	10^0	2	79.6
	10^1	2	96.0
	10^2	3	56.2 ± 36.2
	10^4	3	0.34 ± 0.4

with the results from the RT-PCR and co-culture assays (Table 1).

3.4. Humoral response of MV- and rMV-E1E2-infected hu-PBL-NOJ mice

To examine the immune response against MV and rMV-E1E2 by the transplanted human PBLs, we measured human MV- or HCV-specific antibodies using an ELISA with an MV-infected B95a cell lysate (Fig. 4A) or recombinant HCV E2 protein (Fig. 4B). A significant amount of human antibody against MV antigens was detected in the sera from mice that were infected with MV (10^0–10^1 pfu) or rMV-E1E2 (10^1–10^2 pfu) (Fig. 4A and B). However, only one mouse, which was infected with 10^2 pfu of rMV-E1E2, generated human antibodies against HCV E2 (Fig. 5A). The antibody responses in this mouse were confirmed by Western blot analysis (Fig. 5B).

4. Discussion

The development of a vaccine against HCV has relied on several tools, including recombinant proteins and peptides that are derived from HCV antigens [12,32–34]. HCV E1 E2 proteins play essential roles in the entry of HCV into host cells. Therefore, these proteins represent ideal targets for neutralising antibodies to block viral entry.

Several studies have used the measles virus as a vector for expression of other viral proteins [16,17]. In this study, we examined the infectivity of a rescued Edmonston B strain of MV and a recombinant rMV-E1E2 that was constructed using reverse genetics [25,30]. We demonstrate that these viruses can infect hu-PBL-NOJ mice. This is the first report demonstrating that rescued virus, including a recombinant virus, can infect hu-PBL-NOJ mice. Furthermore, an adequate viral titer could control the generation of antibodies in these mice. Based on the flow cytometry data, most of the human leukocytes disappeared following infection with high virus titer (10^3–10^4 pfu) and human antibody was not detected in these mice (data not shown). In contrast, a population of human leukocytes was detected in the mice that were inoculated with a lower dose of virus (10^0–10^2 pfu). In addition, we could detect human antibodies in the serum of mice that were infected with a low dose of virus, suggesting that this viral titer range is suitable for the induction of an antibody response that targets rMVs in the hu-PBL-NOJ mouse system. This range of virus concentration is adequate for antibody production and the resulting antibody response might suppress the viral growth of 10^0–10^1 pfu MVs in hu-PBL-NOJ mice.

The humanised mouse is a promising model for studying the transmission of the live, attenuated Edmonston B strain of the measles virus. There have been several reports detailing the infection of experimental transgenic mice that

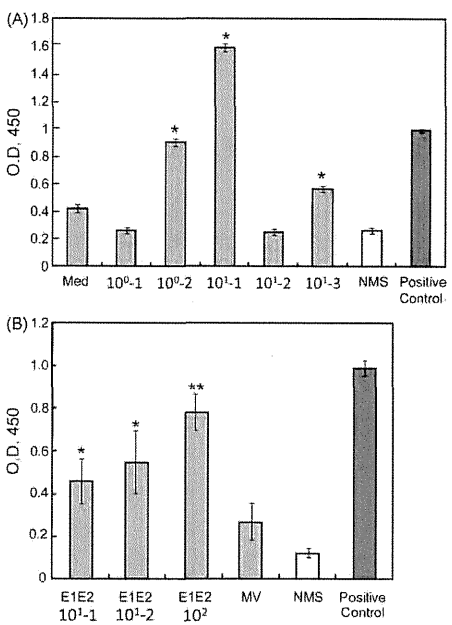

Fig. 4. Detection of human MV-specific antibodies in the serum of rMV- or rMV-E1E2-infected mice. (A) Serum (1:100) from MV-infected mice (10^0–10^1 pfu) was analysed by ELISA using an MV-infected B95a cell lysate as the target. An anti-MV-NP antibody was used as a positive control and NMS indicates normal mouse serum. The asterisk (*) indicates a significant reaction ($p < 0.01$) compared to the medium alone control. (B) Serum (1:100) from rMV-E1E2-infected mice (10^1–10^2 pfu) was analysed by ELISA. An anti-MV-NP antibody was used as a positive control and NMS indicates normal mouse serum. The double asterisk (**) indicates a highly significant reaction ($p < 0.001$) compared to NMS and a single asterisk (*) indicates a significant reaction ($p < 0.05$) compared to NMS.

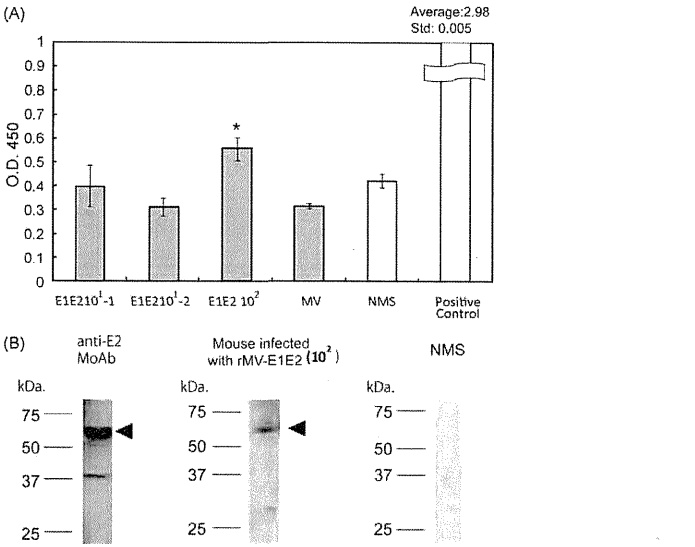

Fig. 5. Detection of E2-specific antibodies using ELISA and western blot. (A) Baculovirus-expressed E2 protein was used as the ELISA antigen and serum (diluted 1:100) from rMV-E1E2-infected mice (10^1–10^2 pfu) was analysed. Anti-E2 monoclonal antibody (MoAb 544) was used as positive control. The asterisk (*) indicates a significant reaction ($p < 0.05$) compared to NMS. (B) An anti-E2 monoclonal antibody (MoAb 544), serum from rMV-E1E2 infected mice (1:100), or normal mouse serum (1:100) was used as primary antibodies in a western blot to detect baculovirus-expressed E2 protein. The triangles indicate bands that correspond to HCV E2.

expresses human CD46 and CD150 with some strains of measles virus [35,36]. However, unlike in other animal models, a population of human cells is the target of the virus in this study. Furthermore, the use of hu-PBL-NOJ mice allows one to monitor the immune response that is generated by human leukocytes against the immunogen. Based on our results, hu-PBL-NOJ mice should be a useful tool for studying the immune response during early MV or rMV-E1E2 infection. Since there is no animal model of HCV infection, monitoring the immune response of human leukocytes permits the accurate evaluation of potential vaccine candidates.

We detected a significant amount of MV-specific antibodies in the rMV-E1E2-infected mice ($n = 3$). However, only one mouse produced E2-specific antibodies and no mice produced E1-specific antibodies. This result could be explained by the hypothesis that the immunogenicity of the E1 and E2, especially E1 protein might be lower than the immunogenicity of the MV proteins, an observation that is consistent with previous studies [37–40].

Further development of the hu-PBL-NOJ mouse model system will allow us to characterise not only the immediate immune response, but also the long-term evolution of the human immune response against measles virus and recombinant measles viruses. This system will make it possible to evaluate the immunogenicity of potential vaccine targets using human PBLs, which is indispensable for the development of an effective vaccine of HCV.

Acknowledgements

We would like to thank Drs. M.A. Billeter and K. Takeuchi for providing the MV Edmonston B strain rescue system, F. Ikeda and M. Yoneda for their technical support. This work was supported by grants from the Ministry of Health and Welfare of Japan, the Ministry of Education, Culture, Sports, Science and Technology of Japan, the Program for Promotion of Fundamental Studies in Health Sciences of the National Institute of Biomedical Innovation, and the Cooperative Research Project on Clinical and Epidemiological Studies of Emerging and Re-emerging Infectious Diseases.

References

[1] Di Bisceglie AM, Carithers Jr RL, Gores GJ. Hepatocellular carcinoma. Hepatology 1998;28(4):1161–5.
[2] Hayashi J, et al. Hepatitis C virus and hepatocarcinogenesis. Intervirology 1999;42(2–3):205–10.
[3] Michielsen PP, Francque SM, van Dongen JL. Viral hepatitis and hepatocellular carcinoma. World J Surg Oncol 2005;3:27.
[4] Global surveillance and control of hepatitis C. Report of a WHO Consultation organized in collaboration with the Viral Hepatitis Prevention Board, Antwerp, Belgium. J Viral Hepat, 1999;6(1):35–47.
[5] Zoulim F, et al. Clinical consequences of hepatitis C virus infection. Rev Med Virol 2003;13(1):57–68.
[6] Bruchfeld A, et al. Ribavirin treatment in dialysis patients with chronic hepatitis C virus infection—a pilot study. J Viral Hepat 2001;8(4):287–92.
[7] Mazzella G, et al. Alpha interferon treatment may prevent hepatocellular carcinoma in HCV-related liver cirrhosis. J Hepatol 1996;24(2):141–7.

[8] Kohara M, et al. Hepatitis C virus genotypes 1 and 2 respond to interferon-alpha with different virologic kinetics. J Infect Dis 1995;172(4):934–8.
[9] Nakamura H, et al. Interferon treatment for patients with chronic hepatitis C infected with high viral load of genotype 2 virus. Hepatogastroenterology 2002;49(47):1373–6.
[10] Bukh J, et al. Studies of hepatitis C virus in chimpanzees and their importance for vaccine development. Intervirology 2001;44(2–3):132–42.
[11] Bowen DG, Walker CM. Mutational escape from CD8+ T cell immunity: HCV evolution, from chimpanzees to man. J Exp Med 2005;201(11):1709–14.
[12] Lechmann M, Liang TJ. Vaccine development for hepatitis C. Semin Liver Dis 2000;20(2):211–26.
[13] Combredet C, et al. A molecularly cloned Schwarz strain of measles virus vaccine induces strong immune responses in macaques and transgenic mice. J Virol 2003;77(21):11546–54.
[14] Naniche D, et al. Decrease in measles virus-specific CD4 T cell memory in vaccinated subjects. J Infect Dis 2004;190(8):1387–95.
[15] Ovsyannikova IG, et al. Frequency of measles virus-specific CD4+ and CD8+ T cells in subjects seronegative or highly seropositive for measles vaccine. Clin Diagn Lab Immunol 2003;10(3):411–6.
[16] Brandler S, et al. Pediatric measles vaccine expressing a dengue antigen induces durable serotype-specific neutralizing antibodies to dengue virus. PLoS Negl Trop Dis 2007;1(3):e96.
[17] Brandler S, Tangy F. Recombinant vector derived from live attenuated measles virus: potential for flavivirus vaccines. Comp Immunol Microbiol Infect Dis 2008;31(2–3):271–91.
[18] Guerbois M, et al. Live attenuated measles vaccine expressing HIV-1 Gag virus like particles covered with gp160DeltaV1V2 is strongly immunogenic. Virology 2009;388(1):191–203.
[19] Liniger M, et al. Recombinant measles viruses expressing single or multiple antigens of human immunodeficiency virus (HIV-1) induce cellular and humoral immune responses. Vaccine 2009;27(25–26):3299–305.
[20] Lorin C, et al. A recombinant live attenuated measles vaccine vector primes effective HLA-A0201-restricted cytotoxic T lymphocytes and broadly neutralizing antibodies against HIV-1 conserved epitopes. Vaccine 2005;23(36):4463–72.
[21] Lorin C, et al. A single injection of recombinant measles virus vaccines expressing human immunodeficiency virus (HIV) type 1 clade B envelope glycoproteins induces neutralizing antibodies and cellular immune responses to HIV. J Virol 2004;78(1):146–57.
[22] Cantarella G, et al. Recombinant measles virus-HPV vaccine candidates for prevention of cervical carcinoma. Vaccine 2009;27(25–26):3385–90.
[23] Liniger M, et al. Induction of neutralising antibodies and cellular immune responses against SARS coronavirus by recombinant measles viruses. Vaccine 2008;26(17):2164–74.
[24] Despres P, et al. Live measles vaccine expressing the secreted form of the West Nile virus envelope glycoprotein protects against West Nile virus encephalitis. J Infect Dis 2005;191(2):207–14.
[25] Radecke F, et al. Rescue of measles viruses from cloned DNA. EMBO J 1995;14(23):5773–84.
[26] Okada S, et al. Early development of human hematopoietic and acquired immune systems in new born NOD/Scid/Jak3null mice intrahepatic engrafted with cord blood-derived CD34+ cells. Int J Hematol 2008;88(5):476–82.
[27] Hattori S, et al. Potent activity of a nucleoside reverse transcriptase inhibitor, 4'-ethynyl-2-fluoro-2'-deoxyadenosine, against human immunodeficiency virus type 1 infection in a model using human peripheral blood mononuclear cell-transplanted NOD/SCID Janus kinase 3 knockout mice. Antimicrob Agents Chemother 2009;53(9):3887–93.
[28] Kobune F, Sakata H, Sugiura A. Marmoset lymphoblastoid cells as a sensitive host for isolation of measles virus. J Virol 1990;64(2):700–5.
[29] Tsukiyama-Kohara K, et al. Activation of the CKI-CDK-Rb-E2F pathway in full genome hepatitis C virus-expressing cells. J Biol Chem 2004;279(15):14531–41.
[30] Yoneda M, et al. Rinderpest virus phosphoprotein gene is a major determinant of species-specific pathogenicity. J Virol 2004;78(12):6676–81.
[31] Op De Beeck A, Cocquerel L, Dubuisson J. Biogenesis of hepatitis C virus envelope glycoproteins. J Gen Virol 2001;82(Pt 11):2589–95.
[32] Beyene A, et al. Hepatitis C virus envelope glycoproteins and potential for vaccine development. Vox Sang 2002;83(Suppl 1):27–32.
[33] Seong YR, et al. Immunogenicity of the E1E2 proteins of hepatitis C virus expressed by recombinant adenoviruses. Vaccine 2001;19(20–22):2955–64.
[34] Stamataki Z, et al. Hepatitis C virus envelope glycoprotein immunization of rodents elicits cross-reactive neutralizing antibodies. Vaccine 2007;25(45):7773–84.
[35] Ohno S, et al. Measles virus infection of SLAM (CD150) knockin mice reproduces tropism and immunosuppression in human infection. J Virol 2007;81(4):1650–9.
[36] Sellin CI, et al. High pathogenicity of wild-type measles virus infection in CD150 (SLAM) transgenic mice. J Virol 2006;80(13):6420–9.
[37] Falkowska E, et al. Hepatitis C virus envelope glycoprotein E2 glycans modulate entry, CD81 binding, and neutralization. J Virol 2007;81(15):8072–9.
[38] Helle F, et al. The neutralizing activity of anti-hepatitis C virus antibodies is modulated by specific glycans on the E2 envelope protein. J Virol 2007;81(15):8101–11.
[39] Jackson P, et al. Reactivity of synthetic peptides representing selected sections of hepatitis C virus core and envelope proteins with a panel of hepatitis C virus-seropositive human plasma. J Med Virol 1997;51(1):67–79.
[40] Hoofnagle JH. Course and outcome of hepatitis C. Hepatology 2002;36(5 Suppl 1):S21–9.

Murakami et al. BMC Medical Genomics 2010, 3:48
http://www.biomedcentral.com/1755-8794/3/48

BMC Medical Genomics

RESEARCH ARTICLE Open Access

Hepatic microRNA expression is associated with the response to interferon treatment of chronic hepatitis C

Yoshiki Murakami[1*], Masami Tanaka[2], Hidenori Toyoda[3], Katsuyuki Hayashi[4], Masahiko Kuroda[2], Atsushi Tajima[5], Kunitada Shimotohno[6]

Abstract

Background: HCV infection frequently induces chronic liver diseases. The current standard treatment for chronic hepatitis (CH) C combines pegylated interferon (IFN) and ribavirin, and is less than ideal due to undesirable effects. MicroRNAs (miRNAs) are endogenous small non-coding RNAs that control gene expression by degrading or suppressing the translation of target mRNAs. In this study we administered the standard combination treatment to CHC patients. We then examined their miRNA expression profiles in order to identify the miRNAs that were associated with each patient's drug response.

Methods: 99 CHC patients with no anti-viral therapy history were enrolled. The expression level of 470 mature miRNAs found their biopsy specimen, obtained prior to the combination therapy, were quantified using microarray analysis. The miRNA expression pattern was classified based on the final virological response to the combination therapy. Monte Carlo Cross Validation (MCCV) was used to validate the outcome of the prediction based on the miRNA expression profile.

Results: We found that the expression level of 9 miRNAs were significantly different in the sustained virological response (SVR) and non-responder (NR) groups. MCCV revealed an accuracy, sensitivity, and specificity of 70.5%, 76.5% and 63.3% in SVR and non-SVR and 70.0%, 67.5%, and 73.7% in relapse (R) and NR, respectively.

Conclusions: The hepatic miRNA expression pattern that exists in CHC patients before combination therapy is associated with their therapeutic outcome. This information can be utilized as a novel biomarker to predict drug response and can also be applied to developing novel anti-viral therapy for CHC patients.

Background

Hepatitis C virus (HCV) infection affects more than 3% of the world population. HCV infection frequently induces chronic liver diseases ranging from chronic hepatitis (CH) C, to liver cirrhosis (LC) and hepatocellular carcinoma (HCC) [1]. The current standard treatment for CHC combines pegylated interferon (Peg-IFN) and ribavirin, and has been found to be effective in only 50% of HCV genotype 1b infection. Furthermore this form of therapy is often accompanied by adverse effects; therefore, there is a pressing need to develop alternative strategies to treat CHC and to identify patients that will not be responsive to treatment [2].

MicroRNAs (miRNAs) are endogenous small non-coding RNAs that control gene expression by degrading or suppressing the translation of target mRNAs [3,4]. There are currently 940 identifiable human miRNAs (The miRBase Sequence Database – Release 15.0). These miRNAs can recognize hundreds of target genes with incomplete complementary over one third of human genes appear to be conserved miRNA targets [5,6]. miRNA can associate not only several pathophysiologic events but also cell proliferation and differentiation.

However, there are many miRNAs whose functions are still unclear. Examples include miR-122 which is an abundant liver-specific miRNA that is said to constitute

* Correspondence: ymurakami@genome.med.kyoto-u.ac.jp
[1]Center for Genomic Medicine, Kyoto University Graduate School of Medicine, 53 Shogoinkawahara-cho, Sakyo-ku, Kyoto 606-8507, Japan
Full list of author information is available at the end of the article

up to 70% of all miRNA molecules in hepatocytes [7]. The expression level of miR-122 was reportedly associated with early response to IFN treatment, while others like miR-26 have expression status that is associated with HCC survival and response to adjuvant therapy with IFN [8,9]. IFN beta (IFNβ) on the other hand, has been shown to rapidly modulate the expression of numerous cellular miRNAs, and it has been demonstrated that 8 IFNβ-induced miRNAs have sequence-predicted targets within the hepatitis C virus (HCV) genomic RNA [10]. Finally several miRNAs have been recognized as having target sites in the HCV genome that inhibits viral replication [10-12].

To date, various parameters have been examined in an attempt to confirm the effects of the IFN-related treatment for CHC. In patients with chronic HCV genotype 1b infection, there is a substantial correlation between responses to IFN and mutation in the interferon sensitivity determining region (ISDR) of the viral genome [13]. Substitutions of amino acid in the HCV core region (aa 70 and aa 91) were identified as predictors of early HCV-RNA negativity and several virological responses, including sustained response to standard combination therapy [14]. In order to assess the drug response to combination therapy for CHC using gene expression signatures, several researchers cataloged the IFN related gene expression profile from liver tissue or peripheral blood mononuclear cells (PBMC) [15,16]. It was found that failed combination therapy was associated with up-regulation of a specific set of IFN-responsive genes in the liver before treatment [17]. Additional reports have indicated that two SNPs near the gene IL28B on chromosome 19 may also be associated with a patient's lack of response to combination therapy [18]. These reports suggest that gene expression during the early phase of anti-HCV therapy may elucidate important molecular pathways for achieving virological response [19].

Our aim in this study was to identify gene related factors that contribute to poor treatment response to combination therapy for CHC. In order to achieve this we studied the miRNA expression profile of CHC patients before treatment with CHC combination therapy and tried to determine the miRNAs that were associated with their drug response. Knowing patients' expression profile is expected to provide a clearer understanding of how aberrant expression of miRNAs can contribute to the development of chronic liver disease as well as aid in the development of more effective and safer therapeutic strategies for CHC.

Methods

Patients and sample preparation

Ninety-nine CHC patients with HCV genotype 1b were enrolled (Table 1). Patients with autoimmune hepatitis, or alcohol-induced liver injury, or hepatitis B virus-associated antigen/antibody or anti-human immunodeficiency virus antibody were excluded. There were no patients who received IFN therapy or immunomodulatory therapy before enrollment in the study. Serum HCV RNA was quantified before IFN treatment using Amplicor-HCV Monitor Assay (Roche Molecular Diagnostics Co., Tokyo, Japan). Liver biopsy specimen was collected from each patient up to one week prior to administering combination therapy. Histological grading and staging of liver biopsy specimens from the CHC patients were performed according to the Metavir classification system. Pretreatment blood tests were conducted to determine each patient's level of aspartate aminotransferase, alanine aminotransferase, total bilirubin, alkaline phosphatase, gamma-glutamyl transpeptidase, white blood cell (WBC), platelets, and hemoglobin. Written informed consent was obtained from all of the patients or their guardians and provided to the Ethics Committee of the Graduate School of Kyoto University, who approved the conduct of this study in accordance with the Helsinki Declaration.

Table 1 Clinical characteristics of patients

Characteristics	SVR (n = 46)	R (n = 28)	NR (n = 25)	p-value
Age (years)	57.0 ± 9.8	61.2 ± 8.3	60.6 ± 7.6	0.09†
Male (%)	28 (61%)	11 (39%)	9 (36%)	0.08§
Weight (kg)	59.5 ± 9.0	56.6 ± 9.9	56.0 ± 7.7	0.13†
HCV RNA ($\times 10^6$ copies/ml)	1.90 ± 1.95	1.83 ± 1.04	1.58 ± 0.93	0.62†
Fibrosis stage				
F 0	1	1	1	0.50§
F 1	29	16	10	
F 2	10	7	6	
F 3	6	4	7	
F 4	0	0	1	
WBC($\times 10^3$/mm^3)	5.31 ± 1.59	5.18 ± 1.24	4.71 ± 1.15	0.29†
Hemoglobin (g/dl)	14.2 ± 1.26	13.6 ± 1.35	13.5 ± 1.13	0.022†
Platelet ($\times 10^4$/mm^3)	16.7 ± 5.0	16.4 ± 4.0	15.2 ± 6.1	0.25†
AST (IU/L)	54.8 ± 48.1	46.6 ± 29.3	57.0 ± 28.5	0.17†
ALT (IU/L)	74.5 ± 87.8	47.9 ± 28.6	67.6 ± 43.2	0.15†
γGTP (IU/L)	56.0 ± 69.4	38.5 ± 28.9	74.3 ± 59.0	0.025†
ALP (IU/L)	248 ± 71.5	245 ± 75.7	323 ± 151	0.038†
Total Bilirubin (mg/dl)	0.67 ± 0.22	0.72 ± 0.30	0.68 ± 0.19	0.95†
Albumin (g/dl)	4.21 ± 0.31	4.13 ± 0.27	4.01 ± 0.48	0.14†

Abbreviations. SVR, sustained virological response; R, relapse; NR, non responder; Differences in clinical characteristics among three groups were tested using †Kruskal-Wallis test, or §Fisher's exact test. AST, aspartate aminotransferase; ALT, alanine aminotransferase; WBC, white blood cell; ALP, alkaline phosphatase; γGTP, gamma-glutamyl transpeptidase.

Treatment protocol and definitions

All enrolled patients were treated with pegylated IFNa-2b (Schering-Plough Corporation, Kenilworth, NJ, USA) and ribavirin (Schering-Plough) for 48 weeks (Figure 1). Pegylated IFN was administered at a dose of 1.5 mg kg/week at the starting point. Ribavirin was administered following the dose recommended by the manufacturer.

Definitions of drug response to therapy

Drug response was defined according to how much HCV RNA had decreased in each patient's serum. After four weeks of drug administration (rapid response phase) the patients were classified into the following two groups after four weeks of drug administration: (i) rapid virological responder (RVR): a patient whose serum was negative for serum HCV RNA at four weeks, and (ii) non-RVR: a patient who was not classified as RVR.

The patients were classified into the following three groups after 12 weeks of drug administration (early response phase): (i) complete early virological responder (cEVR): a patient who was negative for serum HCV RNA at 12 weeks; (ii) partial EVR: a patient whose serum HCV RNA was reduced by 2-log or more of the HCV RNA before drug administration at 12 weeks, but who was not negative for serum HCV RNA; and (iii) non-EVR: a patient who was not classified as either cEVR or pEVR.

The patients were classified into the following three groups at the time of post-treatment at 24 weeks (final response): (i) sustained virological responder (SVR): a patient who was negative for serum HCV RNA during the six months following completion of the combination therapy; (ii) relapse (R): a patient whose serum HCV RNA was negative by the end of the combination therapy but reappeared after completion of the combination therapy; and (iii) virological non-responder (NR): a patient who was positive for serum HCV RNA during the entire course of the combination treatment.

RNA extraction

Liver biopsy specimens were stored in RNA later (Ambion, Austin, TX, USA) at -80°C until RNA

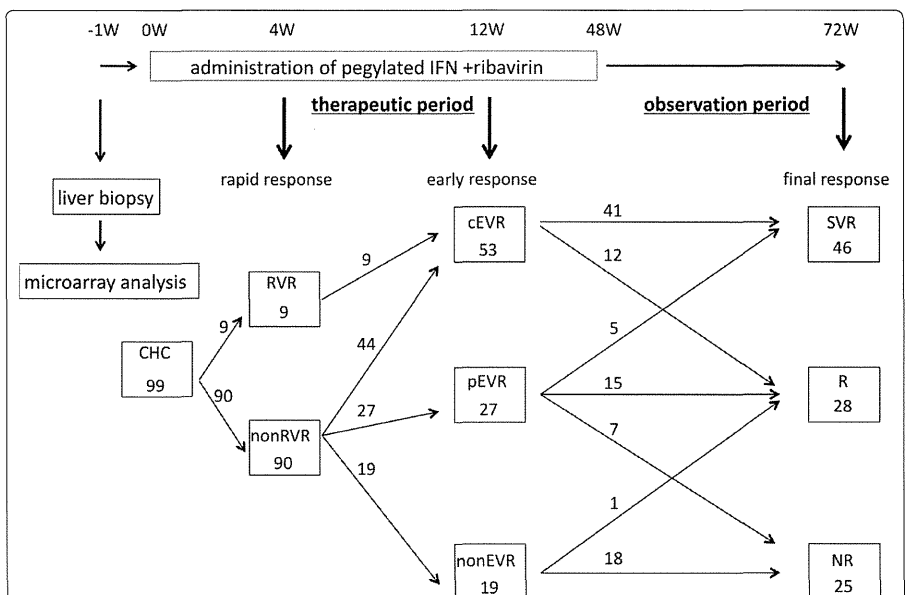

Figure 1 Study design and time-line response to combination therapy. The time-course of liver biopsy, microarray analysis, therapeutic period, observation period after combination therapy, and drug response judgment time (4W, 12W, 72W) is shown. Each therapeutic result (rapid, early, and final response) and the number of patients transitioning into each group are shown. RVR, cEVR, pEVR, SVR, R, and NR are denoted as rapid virological response, complete early virological response, partial EVR, sustained virological response, relapse, and non responder, respectively.

extraction. Total RNA was extracted by using mirVana™ miRNA Isolation kit (Ambion) according to the manufacturer's instruction.

miRNA microarray

miRNA microarrays were manufactured by using Agilent Technologies (Santa Clara, CA, USA). Total RNA (100 ng) were labeled and hybridized using a Human microRNA Microarray kit (Agilent Technologies) according to the manufacturer's protocol (Protocol for use with Agilent microRNA microarrays Version 1.5). Hybridization signals were detected using the DNA microarray scanner G2505B (Agilent Technologies), and all scanned images were analyzed using Agilent feature extraction software (v9.5.3.1). Data were analyzed using GeneSpring GX 7.3.1 software (Agilent Technologies) and normalized as follows: (i) values below 0.01 were set to 0.01. (ii) each measurement was divided by the 75th percentile of all measurements to compare one-color expression profiles. The data presented in this manuscript have been deposited in NCBI's Gene Expression Omnibus and are accessible through GEO Series accession number GSE16922: http://www.ncbi.nlm.nih.gov/geo/query/acc.cgi?token=xlmbxyyumcwkeba&acc=GSE16922

Real-time qPCR for miRNA quantification

To detect the expression level of miRNA by real-time qPCR, TaqMan® microRNA assay (Applied Biosystems) was used to quantify the relative expression levels of miR-18a (assay ID, 002422), miR-27b (assay ID, 000409), miR-422b (assay ID, 000575), miR-143 (assay ID, 000466), miR-145 (assay ID, 000467), miR-34b (assay ID, 000427), miR-378 (assay ID, 000567) and U18 (assay ID, 001204) which was used as an internal control. cDNA was synthesized by Taqman miRNA RT Kit (Applied Biosystems). Total RNA (10 ng) in 5 ul of nuclease free water was added to 3 ul of 5× RT primer, 10× 1.5 ul of reverse transcriptase buffer, 0.15 ul of 100 mM dNTP, 0.19 ul of RNase inhibitor, 4.16 ul of nuclease free water, and 50 U of reverse transcriptase in a total volume of 15 ul. The reaction was performed for 30 min at 16°C, 30 min at 42°C, and five min at 85°C. All RT reactions were run in triplicate. Chromo 4 detector (BIO-RAD, Hercules, CA, USA) was used to detect miRNA expression.

Method of predicting prognosis

Monte Carlo Cross Validation (MCCV) was used to identify a set of prognostic miRNAs and to assess and predict drug response [20,21]. We chose MCCV to make up for relatively small number of patients. The 99 enrolled patients were repeatedly and randomly divided 100 times into training sets (TSs; size n = 10, 20, ..., 90) and a corresponding validation set (VS; size = 99-n). The percentile-normalized measures for miRNA expression were compared between the 2 TS patient groups of SVR and non-SVR (R and NR) by computing absolute values of the difference for each of the 172 miRNAs that were higher than 10. A prognosis signature was defined in terms of the expression measures of the miRNAs with the largest absolute differences. A 35-miRNA prognosis predictor (PP) was established for TS patients and its performance was assessed on VS patients. A PP was computed by applying diagonal linear discriminant analysis to the 35-miRNA PP of the TS patients (Table 2 and 3). The PP was applied to predict the prognoses of the VS patients. The predicted and actual prognoses (SVR or non-SVR) of the VS patients were compared to obtain the following three measures of prognosis prediction performance: (1) accuracy (proportion of correctly predicted prognoses), (2) sensitivity (proportion of correctly predicted non-SVR) and (3) specificity (proportion of correctly predicted SVR). 53 patients (N and NR) were also repeatedly and randomly divided 100 times into training sets (TSs; size n = 6, 12, ...42) and corresponding validation set (VS; size = 53-n). Perl programs of our own writing performed all analytical processes.

Cell lines and miRNA transfection

HEK293 cells were maintained in D-MEM (Invitrogen, Carlsbad, CA, USA) with 10% fetal bovine serum, plated in 60 mm diameter dishes and cultured to 70% confluence. 293 cells were plated in 6-well plates the day before transfection and grown to 70% confluence. Cells were transfected with 50 pmol of Silencer® negative control siRNA (Ambion) or double-stranded mature miRNA (ds miRNA) or 2'-O-methylated antisense oligonucleotide against the miRNA of interest (ASO miRNA) (Hokkaido System Science, Sapporo, Japan) using lipofectamine RNAiMAX (Invitrogen). Cells were harvested 2 days after transfection.

Real-time qPCR for mRNA quaniflcation

cDNA was synthesized using the Transcriptor High Fiderity cDNA synthesis Kit (Roche, Basel, Switzerland). Total RNA (2 μg) in 10.4 μl of nuclease free water was added to 1 μl of 50 mM random hexamer. The denaturing reaction was performed for 10 min at 65°C. The denatured RNA mixture was added to 4 μl of 5× reverse transcriptase buffer, 2 μl of 10 mM dNTP, 0.5 μl of 40 U/μl RNase inhibitor, and 1.1 μl of reverse transcriptase (FastStart Universal SYBR Green Master (Roche) in a total volume of 20 μl. The reaction ran for 30 min at 50° C (cDNA synthesis), and five min at 85°C (enzyme denaturation). All reactions were run in triplicate. Chromo 4 detector (BIO-RAD, Hercules, CA, USA) was used to detect mRNA expression. The primer sequences are as follows; BCL2 s; 5'-gttgctttacgtggcctgtt-3', as; 5'-ggaggtctggcttcatacca-3', RARA s; 5'-catacctgccataccaacc-3', as; 5'-gacatgaaaggagagtgggg-3', SMAD2 s; 5'-aatattttggggactgatgcc-3', as; 5'-gcttttgggcagtggttaag-3', and β-actin s; 5'-ccactggcatcgtgatggac-3', as; 5'-tcattgccaatggtgatgacct-3'. Assays were performed in triplicate, and the expression levels of target genes were normalized to the expression of the β-actin gene, as quantified using real-time qPCR as internal controls.

Statistical analysis

Data were statistically analyzed using the Student's t-test and differences in clinical characteristics among 3 groups were tested using the Kruskal-Wallis test, or Fisher's exact test. Data from microarray were also statically analyzed using Welch's test and Benjamini-Hochberg correction for multiple hypotheses testing.

Table 2 List of the 35 miRNAs used to classify patients into SVR and non-SVR groups using Monte Carlo Cross Validation (MCCV)

Gene name	fold change (SVR/non SVR)	T-test	Selection by MCCV		
			Rank	appearance frequency in this classification (%)	appearance number of times
hsa-miR-122a	1.32	6.67E-02	1	98.78	889
hsa-miR-21	1.19	3.62E-01	2	94.67	852
hsa-miR-22	1.23	7.80E-02	3	93.22	839
hsa-let-7a	1.14	3.57E-01	4	92.33	831
hsa-miR-23b	1.41	1.72E-02	5	91.44	823
hsa-miR-26a	1.32	7.45E-02	6	90.78	817
hsa-let-7f	1.15	4.04E-01	7	88.67	798
hsa-miR-142-3p	1.39	1.45E-01	8	87.33	786
hsa-miR-494	2.18	5.85E-03	9	82.00	738
hsa-miR-194	1.22	1.70E-01	10	80.78	727
hsa-let-7b	1.11	3.59E-01	11	80.22	722
hsa-miR-148a	1.25	2.28E-01	12	79.67	717
hsa-miR-29a	1.16	2.73E-01	13	77.78	700
hsa-miR-125b	1.20	2.37E-01	14	73.11	658
hsa-miR-192	1.09	4.89E-01	15	69.67	627
hsa-miR-24	1.25	8.31E-02	16	68.89	620
hsa-miR-768-3p	1.19	1.78E-01	17	68.78	619
hsa-miR-126	1.07	6.75E-01	18	49.56	446
hsa-miR-19b	1.15	2.98E-01	19	48.89	440
hsa-miR-370	2.00	1.44E-02	20	39.00	351
hsa-miR-29c	1.26	1.37E-01	21	38.89	350
hsa-miR-16	1.24	2.08E-01	22	37.11	334
hsa-miR-145	1.01	9.25E-01	23	34.89	314
hsa-let-7c	1.21	1.41E-01	24	33.22	299
hsa-miR-215	1.20	3.65E-01	25	27.67	249
hsa-let-7g	1.16	3.64E-01	26	27.44	247
hsa-miR-451	1.13	6.94E-01	27	23.11	208
hsa-miR-26b	1.30	2.26E-01	28	22.22	200
hsa-miR-92	1.12	3.44E-01	29	21.11	190
hsa-miR-29b	1.19	2.62E-01	30	19.44	175
hsa-miR-107	1.21	1.58E-01	31	18.78	169
hsa-miR-27b	1.40	2.32E-02	32	18.11	163
hsa-miR-638	1.32	5.57E-02	33	16.89	152
hsa-miR-199a*	1.12	5.92E-01	34	16.78	151
hsa-miR-193b	1.25	7.24E-02	35	16.67	150

Results

A microarray platform was used to determine miRNA expression of 470 miRNAs in 99 fresh-frozen CHC liver tissues.

miRNAs which related to the final response of combination therapy

Unique miRNA expression patterns were established according to the final virological response (SVR, R, and NR) to the combination therapy (Figure 1). To isolate

Table 3 List of the miRNAs used to classify patients into R and NR groups

Gene name	fold change (R/NR)	T-test	Selection by MCCV		
			Rank	appearance frequency in this classification (%)	appearance number of times
hsa-miR-122a	1.50	6.70E-02	1	98.57	690
hsa-miR-21	1.13	5.43E-01	2	89.86	629
hsa-let-7a	1.15	4.23E-01	3	88.71	621
hsa-let-7f	1.24	3.01E-01	4	87.43	612
hsa-miR-148a	1.70	4.51E-02	5	82.71	579
hsa-miR-192	1.24	1.93E-01	6	81.71	572
hsa-miR-126	1.21	3.19E-01	7	74.14	519
hsa-miR-22	1.04	7.88E-01	8	68.43	479
hsa-miR-194	1.20	3.63E-01	9	64.29	450
hsa-miR-23b	1.30	2.06E-01	10	62.00	434
hsa-miR-125b	1.23	2.88E-01	11	61.86	433
hsa-miR-494	0.45	8.17E-02	12	61.14	428
hsa-miR-19b	1.17	3.86E-01	13	61.14	428
hsa-miR-29a	1.11	5.44E-01	14	59.86	419
hsa-miR-26a	1.13	5.38E-01	15	58.43	409
hsa-let-7b	1.01	9.37E-01	16	56.86	398
hsa-miR-142-3p	1.15	5.54E-01	17	52.71	369
hsa-miR-215	1.28	3.93E-01	18	52.00	364
hsa-miR-101	1.31	1.26E-01	19	49.00	343
hsa-miR-451	1.35	5.25E-01	20	48.14	337
hsa-miR-145	0.99	9.76E-01	21	47.14	330
hsa-let-7g	1.15	4.84E-01	22	44.00	308
hsa-miR-29c	1.23	2.94E-01	23	43.71	306
hsa-miR-26b	1.37	2.85E-01	24	43.14	302
hsa-miR-768-3p	1.00	9.91E-01	25	36.29	254
hsa-let-7c	1.16	3.76E-01	26	36.14	253
hsa-miR-370	0.43	7.36E-02	27	35.57	249
hsa-miR-92	1.07	6.65E-01	28	34.14	239
hsa-miR-16	1.11	6.18E-01	29	26.71	187
hsa-miR-29b	1.14	5.19E-01	30	25.71	180
hsa-miR-27b	1.40	1.15E-01	31	25.71	180
hsa-miR-24	1.08	6.56E-01	32	20.57	144
hsa-miR-107	1.00	9.81E-01	33	19.57	137
hsa-miR-143	0.95	7.99E-01	34	18.43	129
hsa-miR-214	0.85	3.61E-01	35	17.86	125

the miRNAs that were associated with the drug response to the combination therapy, we chose miRNAs which had ≥ 1.25 fold difference in the mean values of the gene expression level between at least two groups ($p < 0.05$). Unsupervised hierarchical clustering based on all the miRNAs spotted on the chip, revealed a marked, very distinct separation according to the patients' final response of the CHC liver tissue to the Peg-IFN and ribavirin combination therapy (Figure 2).

The result was that the expression level of 3 miRNAs (miR-27b, miR-378, miR-422b) in SVR was significantly higher than that in NR, whereas the expression level of 5 miRNAs (miR-34b, miR-145, miR-143, miR-652, and miR-18a) in SVR was significantly lower than that in NR. Without FDR correction, the expression level of miR-122 in NR was lower than that in SVR. The expression level of 2 miRNAs in SVR was significantly higher than that in R, whereas the expression level of 10 miRNAs in SVR was significantly lower than in that in R. Additionally, the expression level of miR-148a in R was significantly higher than that in NR. There was no significant difference in the expression level of miR-122 in NR and R (Table 4).

Validation of the microarray result by real-time qPCR

The three miRNAs (miR-18a, miR-27b, and miR-422b) with the smallest difference of fold change between NR and SVR groups and four miRNA (miR-143, miR-145, miR-34b, and miR-378) with the largest difference of fold change between NR and SVR groups were chosen to confirm the microarray results using stem-loop based real-time qPCR. The result of real-time qPCR corresponded to the result from the microarray analysis (Figure 3).

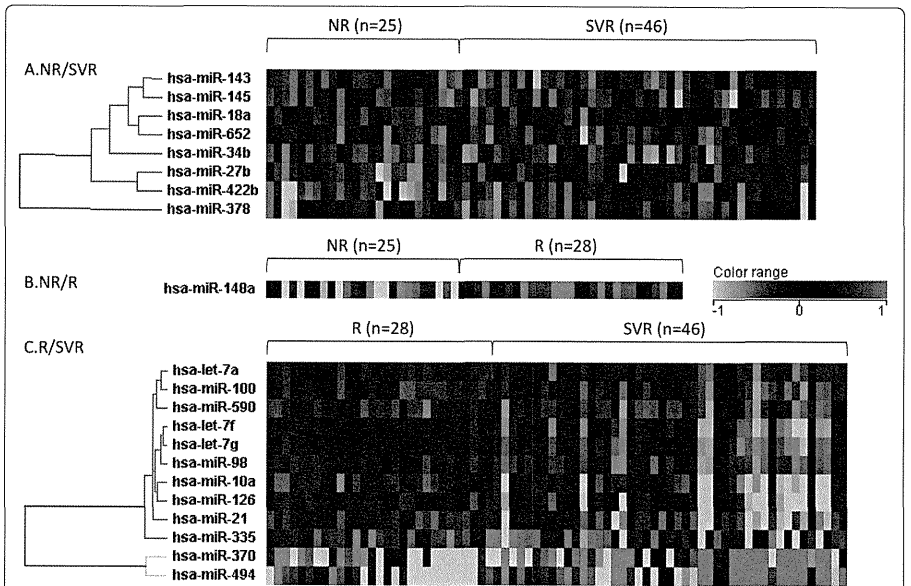

Figure 2 Clustering of CHC patients according to their final response to Peg-IFN and ribavirin combination therapy. Heatmap using miRNA differently expressed among SVR, R, and NR is shown (A: classification between NR and SVR, B: classification between NR and R, and C: classification between R and SVR, respectively). Vertical bars represent the miRNA genes and the horizontal bars represent the samples. Green bars reflect downregulated genes and red bars upregulated genes.

miRNAs which related to the 4 week (rapid response phase) response to combination therapy

The miRNA expression profile was established according to the rapid phase response to the combination therapy by week 4 (Table 5). Our results showed that the expression level of 5 miRNAs in non-RVR was significantly higher than that in RVR. Prior results have revealed that a patient who achieves RVR as a result of the combination therapy has a high possibility of achieving SVR [22,23]. Our research supports this finding: nine out of 99 patients achieved RVR. All nine cases shifted to cEVR by week 12, and 8 shifted to SVR at the final response. The 90 cases in non-RVR shifted to 44 cases in cEVR, 19 in pEVR, and 27 in non-EVR and at the final response shifted to 38 cases in SVR, 27 in R, and 25 in NR (Table 6 and Figure 1).

miRNAs which related to the 12 week (early response phase) response to combination therapy

Establishing the miRNA expression profile of patients according to their 12 week (early response) of CHC liver specimen to the combination therapy after 12 weeks, showed that the expression level of miR-23b and miR-422b in cEVR was higher than that in non-EVR, and the expression level of miR-34b in cEVR lower than that in non-EVR (Table 5). There were no miRNAs with expression level that differed significantly between cEVR and pEVR, and non-EVR and pEVR. The drug response at 12 weeks appeared to be a predictive factor of the final drug response. The 53 cases in cEVR at week 12 shifted to 41 cases in SVR and 12 in R at the final response. 27 cases in pEVR at week 12, shifted to 5 in SVR, 15 in R, and 7 in NR and 19 in non-EVR shifted to 1 in R and 18 in NR (Table 6 and Figure 1).

Predicting the final outcome before drug administration using MCCV

Before initial drug administration, we attempted to simulate the clinical outcome of the combination

Table 4 Extracted miRNA related to the final outcome of combination therapy

Gene Name	Fold Change (NR/SVR)	p-value with FDR correction	p-value without correction
hsa-miR-34b*	1.50	3.53E-02	6.95E-05
hsa-miR-145	1.35	3.55E-02	5.50E-05
hsa-miR-143	1.31	4.65E-02	6.46E-04
hsa-miR-652	1.28	4.33E-02	3.43E-04
hsa-miR-18a	1.22	4.33E-02	2.02E-05
hsa-miR-27b	0.78	4.33E-02	3.97E-05
hsa-miR-422b*	0.71	4.33E-02	1.44E-04
hsa-miR-378	0.70	4.86E-02	1.38E-03
hsa-miR-122	0.72	> 5.00E-02	2.59E-04

Gene Name	Fold Change (NR/R)	p-value with FDR correction	p-value without correction
hsa-miR-148a	0.59	1.60E-02	8.99E-04
has-miR-122	0.72	> 5.00E-02	6.23E-04

Gene Name	Fold Change (R/SVR)	P-value	p-value without correction
hsa-let-7a	1.15	3.93E-02	1.94E-03
hsa-let-7f	1.24	1.04E-02	3.60E-03
hsa-let-7g	1.17	1.93E-02	1.82E-02
hsa-miR-100	1.23	1.93E-02	9.23E-04
hsa-miR-10a	1.37	1.26E-02	2.40E-03
hsa-miR-126	1.36	1.04E-02	1.50E-03
hsa-miR-21	1.30	4.78E-02	3.45E-02
hsa-miR-335	2.00	2.83E-02	3.50E-02
hsa-miR-370	0.36	1.38E-02	2.96E-03
hsa-miR-494	0.37	3.93E-02	1.97E-03
hsa-miR-590	1.26	3.93E-02	5.59E-03
hsa-miR-98	1.22	1.38E-02	6.64E-03

Asterisk was denoted the common miRNAs appeared whose expression level between NR and SVR, and nonEVR and cEVR.

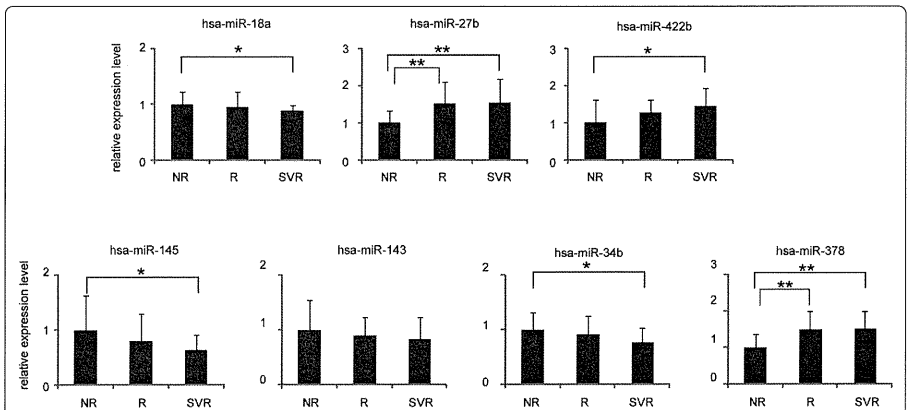

Figure 3 Real-time qPCR validation of the seven miRNAs. Each column represents the relative amount of miRNAs normalized to expression level of U18. The data shown were means+SD of three independent experiments. Asterisk indicates a significant difference of $p < 0.05$ (*) or $p < 0.01$ (**).

Table 5 List of the miRNA related to the rapid or early outcome of combination therapy

Gene Name	Fold Change (non RVR/RVR)	p-value	p-value without correction
hsa-let-7c	1.17	2.01E-02	8.31E-03
hsa-let-7d	1.13	3.50E-02	5.63E-02
hsa-miR-139	1.29	3.35E-02	2.70E-02
hsa-miR-324-5p	1.14	1.64E-02	3.24E-02
hsa-miR-768-5p	1.34	4.57E-02	1.29E-02

Gene Name	Fold Change (non EVR/cEVR)	p-value	p-value without correction
hsa-miR-34b*	1.51	3.30E-02	1.69E-04
hsa-miR-23b	0.74	2.69E-02	8.91E-05
hsa-miR-422b*	0.67	2.40E-02	1.34E-04
hsa-miR-122	0.74	> 5.00E-02	3.07E-03

Asterisk was denoted the common miRNAs appeared whose expression level between NR and SVR, and nonEVR and cEVR.

therapy before drug administration by using MCCV. We first extracted the SVR and non-SVR groups from all of the patients, and then the R and NR groups were predicted afterwards. MCCV simulation showed that the accuracy, specificity, and sensitivity of the liver specimen classified as SVR or non-SVR was up to 70.5%, 63.3%, and 76.8%, respectively (TSs = 80). On the other hand, the accuracy, specificity, and sensitivity of the liver specimen classified as R or NR was 70.0%, 73.7%, and 67.5%, respectively (TSs = 42)(Figure 4). Fold change of their normalized expression level, P value, and number of selection by MCCV in the 35 informative miRNAs that were identified based on the all patients are shown in Table 2 and 3.

miRNAs related to the final drug response can regulate the immune related genes

In order to clarify the biological links between miRNAs and IFN responses, we examined whether the expression of immune-related hypothetical miRNAs target genes (additional file 1) could be controlled by miRNAs which were related to the final drug response. We observed the changes in expression level of B-cell CLL/lymphoma 2 (BCL2), retinoic acid receptor, alpha (RARA), and SMAD family member 2 (SMAD2) by real-time qRT-PCR as the expression level of miRNAs (miR-143, miR-27b, and miR-18a) was modified, respectively, in HEK293 cells. The expression level of the hypothetical targets examined was down-regulated by over-expression of the corresponding miRNA and the corresponding antisense oligonucleotide (ASO) inhibited the function of miRNA (additional file 2).

Discussion

Our large and comprehensive screening revealed that hepatic miRNA expression can be associated with a patient's drug response. There are several reports that miRNAs are closely related to innate immunity, and in this study, we found that several miRNAs had the potential to recognize immuno-related genes as target candidates [24-26]. For example, the following hypothetical candidate genes of miR-378, miR-18a, miR-27b, miR-34b, and miR-145 each identified as target genes, Interferon Response Factor (IRF) 1, IRF2, IRF4, IRF6, and IRF7, respectively (additional file 1). Past reports show that miR-422b was related to the B cell differentiation [27]. When an immuno-reaction induces aberrant expression of miRNA, the expression level of miR-34b significantly decreased in H69 cells following IFN-γ stimulation [28]. Bcl-6 positively directs follicular helper T cell differentiation, through combined repression of miR-18a and miR-27b and transcription factors [29].

In our study, there was significant difference in the fold change of the expression level of miRNA based on the drug response, however, the absolute value of the fold change was not so significant (Table 4). Usually one miRNA can regulate many genes including immuno-related gene (additional file 1), and these genes in turn can synergistically affect immune activity. In our preliminary study (additional file 2) BCL-2, RARA, and SMAD2 can be regulated by miR-143, miR-18a, and miR-27b, respectively. Considering that the expression level of several miRNAs changed these minute changes taken together can have a significant impact on a patient's drug-response and innate immunity.

Aberrant expression of miRNA can modify the replication of HCV. According to Vita algorithm, several miRNAs, related to drug response, can recognize HCV genotype 1b sequence as a target (additional file 3) [30]. For example, miR-199a* is able to target the HCV genome and inhibit viral replication [12]. IFN has the ability to modulate expression of certain miRNAs that may either target the HCV RNA genome (miR-196 or miR-

Table 6 Patients' periodical drug response changes

code No.	4W treatment (rapid response)	12W treatment (early response)	48W treatment +24W observation (final outcome)	code No	4W treatment (rapid response)	12W treatment (early response)	48W treatment +24W observation (final outcome)
OCH-105	non RVR	non EVR	NR	OCH-103	RVR	cEVR	SVR
OCH-111	non RVR	pEVR	NR	OCH-104	non RVR	cEVR	SVR
OCH-118	non RVR	non EVR	NR	OCH-107	non RVR	cEVR	SVR
OCH-119	non RVR	non EVR	NR	OCH-108	non RVR	cEVR	SVR
OCH-122	non RVR	pEVR	NR	OCH-109	non RVR	cEVR	SVR
OCH-123	non RVR	non EVR	NR	OCH-110	non RVR	cEVR	SVR
OCH-126	non RVR	non EVR	NR	OCH-112	non RVR	pEVR	SVR
OCH-127	non RVR	non EVR	NR	OCH-114	RVR	cEVR	SVR
OCH-132	non RVR	pEVR	NR	OCH-116	non RVR	cEVR	SVR
OCH-137	non RVR	non EVR	NR	OCH-121	non RVR	pEVR	SVR
OCH-140	non RVR	pEVR	NR	OCH-124	non RVR	cEVR	SVR
OCH-142	non RVR	non EVR	NR	OCH-130	non RVR	cEVR	SVR
OCH-144	non RVR	pEVR	NR	OCH-131	non RVR	cEVR	SVR
OCH-145	non RVR	non EVR	NR	OCH-136	non RVR	cEVR	SVR
OCH-192	non RVR	non EVR	NR	OCH-138	non RVR	cEVR	SVR
OCH-204	non RVR	non EVR	NR	OCH-139	non RVR	cEVR	SVR
OCH-205	non RVR	non EVR	NR	OCH-143	non RVR	cEVR	SVR
OCH-206	non RVR	non EVR	NR	OCH-150	non RVR	cEVR	SVR
OCH-207	non RVR	non EVR	NR	OCH-153	non RVR	cEVR	SVR
OCH-208	non RVR	non EVR	NR	OCH-154	non RVR	cEVR	SVR
OCH-209	non RVR	pEVR	NR	OCH-155	non RVR	cEVR	SVR
OCH-210	non RVR	non EVR	NR	OCH-156	non RVR	cEVR	SVR
OCH-211	non RVR	non EVR	NR	OCH-157	non RVR	pEVR	SVR
OCH-223	non RVR	non EVR	NR	OCH-158	non RVR	pEVR	SVR
OCH-242	non RVR	pEVR	NR	OCH-160	non RVR	cEVR	SVR
OCH-101	non RVR	cEVR	R	OCH-186	non RVR	cEVR	SVR
OCH-102	RVR	cEVR	R	OCH-187	non RVR	cEVR	SVR
OCH-106	non RVR	non EVR	R	OCH-189	non RVR	pEVR	SVR
OCH-113	non RVR	pEVR	R	OCH-190	non RVR	cEVR	SVR
OCH-115	non RVR	cEVR	R	OCH-191	RVR	cEVR	SVR
OCH-117	non RVR	cEVR	R	OCH-194	non RVR	cEVR	SVR
OCH-120	non RVR	pEVR	R	OCH-195	non RVR	cEVR	SVR
OCH-125	non RVR	pEVR	R	OCH-222	non RVR	cEVR	SVR
OCH-128	non RVR	pEVR	R	OCH-228	non RVR	cEVR	SVR
OCH-129	non RVR	pEVR	R	OCH-229	RVR	cEVR	SVR
OCH-133	non RVR	pEVR	R	OCH-230	non RVR	cEVR	SVR
OCH-134	non RVR	pEVR	R	OCH-231	non RVR	cEVR	SVR
OCH-135	non RVR	cEVR	R	OCH-232	non RVR	cEVR	SVR
OCH-141	non RVR	cEVR	R	OCH-233	non RVR	cEVR	SVR
OCH-151	non RVR	pEVR	R	OCH-234	RVR	cEVR	SVR
OCH-152	non RVR	pEVR	R	OCH-236	non RVR	cEVR	SVR
OCH-159	non RVR	pEVR	R	OCH-237	non RVR	cEVR	SVR
OCH-188	non RVR	cEVR	R	OCH-238	non RVR	cEVR	SVR
OCH-213	non RVR	cEVR	R	OCH-240	RVR	cEVR	SVR
OCH-214	non RVR	pEVR	R	OCH-241	RVR	cEVR	SVR
OCH-215	non RVR	pEVR	R	OCH-243	RVR	cEVR	SVR
OCH-216	non RVR	cEVR	R				
OCH-217	non RVR	pEVR	R				
OCH-218	non RVR	cEVR	R				

Table 6: Patients?'? periodical drug response changes *(Continued)*

OCH-219	non RVR	pEVR	R
OCH-220	non RVR	cEVR	R
OCH-221	non RVR	pEVR	R
OCH-239	non RVR	cEVR	R

448) or markedly enhance its replication (miR-122) [10,11]. The low expression level of miR-122 in the subjects shown in the NR group is in accordance with our results, however, after miRNA expression profile with FDR correction, the expression level of miR-122 was not significantly different between SVR and NR groups [8]. One reason why this difference is that their study comprised of patients infected with HCV genotype from 1 to 4 while this study consisted of HCV genotype 1b patients only.

The expression pattern of mRNA in HCV infected liver tissue is different from that of healthy tissue [15]. The expression pattern of the IFN-related genes in liver tissue before administering of IFN therapy, also differs according to the drug response [15,19]. The amount of plasmacytoid dendritic cell (pDC), which are the most potent secretors of antiviral Type-I IFN, has been shown to decrease in the peripheral blood of patients, however, pDC tend to become trapped in the liver tissue if HCV infection is present [31,32]. Taken together, it is possible that the variation in the miRNA expression pattern according to the drug response existed even before therapy.

Previously, large randomized controlled trials of IFN therapy for CHC, identified at pre-treatment stage several possible factors which are associated with the final virological response. These factors include: genotype, amount of HCV RNA in peripheral blood, degree of fibrosis, age, body weight, ethnicity, and steatosis [33]. Viral genome mutation in the ISDR region and the

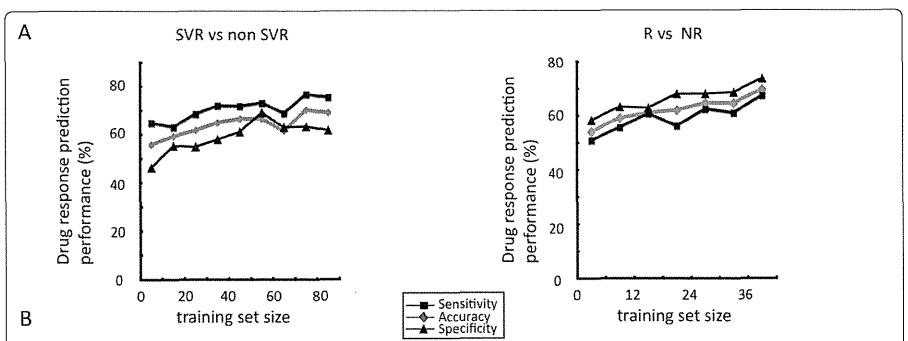

Training	Validation	Accuracy(%)	Sensitivity(%)	Specificity(%)	miRNA_Number
10	89	56.10	65.06	46.31	23
20	79	59.54	63.32	55.38	34
30	69	62.00	68.61	54.91	14
40	59	65.22	72.09	57.93	17
50	49	66.80	71.92	61.12	17
60	39	66.77	73.26	69.07	15
70	29	61.72	68.98	62.99	30
80	19	70.47	76.82	63.31	18
90	9	69.22	75.52	61.72	18

Training	Validation	Accuracy(%)	Sensitivity(%)	Specificity(%)	miRNA_Number
6	48	54.31	51.03	58.29	5
12	42	59.33	55.75	63.24	22
18	36	61.31	60.87	62.87	34
24	30	62.23	56.31	68.07	11
30	24	64.96	62.52	68.09	18
36	18	64.89	61.17	68.69	24
42	12	70.00	67.53	73.73	26

Figure 4 Method for predicting the clinical outcome using MCCV. Prediction performance of signatures from 35 miRNAs (Table 2 and 3). Left: Mean accuracy, specificity, and sensitivity (% in vertical axis) as a function of the training set size were determined for the 100 random splits of patients (non-SVR (NR+R) vs. SVR). Right: prediction performance of the training set size was determined by performing 48 random splits of patients (NR vs. R). A. Prediction performance (mean accuracy, specificity, and sensitivity) and number of miRNAs which was used for the prediction are also shown in each training set (TS) and validation set (VS).

substitutions of amino acid in the HCV core region also served as predictors of early, as well as end-of treatment response [13,14]. The miRNA expression obtained from the therapeutic response, can be applied to the prediction of drug response. The advantages of using miRNA for the microarray analysis include the following; (i) It was relatively easy to analyze because fewer probes were installed compared with the usual cDNA array. (ii) The change in each manifestation of a miRNA was low, in fact, in most miRNA, standard deviation was twice or less in average value (data not shown). The expression levels of miR-34b and 422b in the early response phase and final responses to treatment were consistently and significantly high and low in non-responders, respectively. Therefore these two miRNAs may be useful markers for early-to-final drug response to the IFN treatment.

Further studies are indeed needed to clarify the connection between miRNA expression and patient response to CHC combination therapy. Because information on miRNA is regularly being updated, we are planning to performed more analysis using the latest microarray and a larger sample in the future. However, in the meantime, as we have shown in Figure 4, the bigger the size of the training set, the higher the prediction performance that is achieved. This combined with the results of our Monte Carlo cross validation provided a strong based to verify the concepts in this report. We believe that our results have three advantages (i) the prediction methods used were quite reasonable, (ii) the prediction performance can later be improved if more patients' data become available and (iii) obtaining miRNA profile (not specific miRNAs) is useful for predicting the drug response. While current therapy is based on positive selection with HCV genotype or negative selection with IL28B SNP, and is limited to only some cases, our methods are applicable to all patients [13,18].

Conclusions

Our study shows that the specific miRNA are expressed differently depending on patient's drug response. As result we feel that miRNA profiling can be useful for predicting patient drug response before the administering combination therapy thereby reducing ineffective treatments. Moreover, miRNA expression profile can facilitate the accumulation of basal information for the development of novel therapeutic strategies. This approach allows for more suitable therapeutic strategies based on clinical information of individuals.

Additional material

Additional file 1: miRNA hypothetical target genes according to in silico analysis.

Additional file 2: Real-time qPCR validation of immune-related hypothetical target genes of miRNAs. The expression levels of hypothetical target genes in HEK293 cells were compared among three groups treated with control RNA, ds miRNA, and ASO miRNA. The data shown are means+SD of three independent experiments. Asterisk indicates a significant difference of $p < 0.05$.

Additional file 3: human miRNA target on the HCV genome genotype 1b (Accession No. AF333324)

List of abbreviations

HCV: hepatitis C virus; CH: chronic hepatitis C; LC: liver cirrhosis; HCC: hepatocellular carcinoma; miRNA: microRNA; IFN, interferon; SVR: sustained virological responder; R: relapse; NR: non-responder; RVR: rapid virological responder; EVR: early virological responder.

Acknowledgements

YM and KS were financially supported by the Ministry of Health, Labour and Welfare of Japan. They also received Grants-in-Aid for scientific research from the Ministry of Education, Culture, Sports, Science and Technology. MKwas financially supported by the 'Strategic Research-Based Support' Project for private universities; with matching funds from the Ministry of Education, Culture, Sports, Science and Technology.

Author details

[1]Center for Genomic Medicine, Kyoto University Graduate School of Medicine, 53 Shogoinkawahara-cho, Sakyo-ku, Kyoto 606-8507, Japan. [2]Department of Molecular Pathology, Tokyo Medical University, 6-1-1 Shinjuku, Shinjuku-ku, Tokyo 160-8402, Japan. [3]Department of Gastroenterology, Ogaki Municipal Hospital, 86-4 Minaminokawa-cho, Ogaki, Gifu 503-8502, Japan. [4]DNA Chip Research Inc., 43-1-1 Suehiro-cho, Tsurumi-ku, Yokohama, Kanagawa 230-0045, Japan. [5]Department of Molecular Life Science, Tokai University School of Medicine, 143 Shimokasuya, Isehara, Kanagawa 259-1193, Japan. [6]Research Institute, Chiba Institute for Technology, 2-17-1 Tsudanuma, Narashino, Chiba 275-0016, Japan.

Authors' contributions

YM and KS conceived and designed the experiments; YM, HT and KH performed the experiments; MT and MK performed statistical analysis; YM, MT, HT and AT contributed to writing and editing the manuscript. All authors read and approved the manuscript.

Competing interests

The authors declare that they have no competing interests.

Received: 13 June 2010 Accepted: 22 October 2010
Published: 22 October 2010

References

1. Guidotti LG, Chisari FV: **Immunobiology and pathogenesis of viral hepatitis.** *Annu Rev Pathol* 2006, 1:23-61.
2. Fried MW, Shiffman ML, Reddy KR, Smith C, Marinos G, Goncales FL, Haussinger D, Diago M, Carosi G, Dhumeaux D, Craxi A, Lin A, Hoffman J, Yu J: **Peginterferon alfa-2a plus ribavirin for chronic hepatitis C virus infection.** *N Engl J Med* 2002, **347(13)**:975-982.
3. Ambros V: **The functions of animal microRNAs.** *Nature* 2004, **431(7006)**:350-355.
4. Nilsen TW: **Mechanisms of microRNA-mediated gene regulation in animal cells.** *Trends Genet* 2007, **23(5)**:243-249.
5. Zamore PD, Haley B: **Ribo-gnome: the big world of small RNAs.** *Science (New York, NY)* 2005, **309(5740)**:1519-1524.
6. Pillai RS: **MicroRNA function: multiple mechanisms for a tiny RNA?** *RNA (New York, NY)* 2005, **11(12)**:1753-1761.
7. Lagos-Quintana M, Rauhut R, Yalcin A, Meyer J, Lendeckel W, Tuschl T: **Identification of tissue-specific microRNAs from mouse.** *Curr Biol* 2002, **12(9)**:735-739.

8. Sarasin-Filipowicz M, Krol J, Markiewicz I, Heim MH, Filipowicz W: **Decreased levels of microRNA miR-122 in individuals with hepatitis C responding poorly to interferon therapy.** *Nat Med* 2009, **15(1)**:31-33.
9. Ji J, Shi J, Budhu A, Yu Z, Forgues M, Roessler S, Ambs S, Chen Y, Meltzer PS, Croce CM, Qin LX, Man K, Lo CM, Lee J, Ng IO, Fan J, Tang ZY, Sun HC, Wang XW: **MicroRNA expression, survival, and response to interferon in liver cancer.** *N Engl J Med* 2009, **361(15)**:1437-1447.
10. Pedersen IM, Cheng G, Wieland S, Volinia S, Croce CM, Chisari FV, David M: **Interferon modulation of cellular microRNAs as an antiviral mechanism.** *Nature* 2007, **449(7164)**:919-922.
11. Jopling CL, Yi M, Lancaster AM, Lemon SM, Sarnow P: **Modulation of hepatitis C virus RNA abundance by a liver-specific MicroRNA.** *Science (New York, NY)* 2005, **309(5740)**:1577-1581.
12. Murakami Y, Aly HH, Tajima A, Inoue I, Shimotohno K: **Regulation of the hepatitis C virus genome replication by miR-199a(*).** *J Hepatol* 2009, **50(3)**:453-460.
13. Enomoto N, Sakuma I, Asahina Y, Kurosaki M, Murakami T, Yamamoto C, Ogura Y, Izumi N, Marumo F, Sato C: **Mutations in the nonstructural protein 5A gene and response to interferon in patients with chronic hepatitis C virus 1b infection.** *N Engl J Med* 1996, **334(2)**:77-81.
14. Akuta N, Suzuki F, Kawamura Y, Yatsuji H, Sezaki H, Suzuki Y, Hosaka T, Kobayashi M, Kobayashi M, Arase Y, Ikeda K, Miyakawa Y, Kumada H: **Prediction of response to pegylated interferon and ribavirin in hepatitis C by polymorphisms in the viral core protein and very early dynamics of viremia.** *Intervirology* 2007, **50(5)**:361-368.
15. Asselah T, Bieche I, Narguet S, Sabbagh A, Laurendeau I, Ripault MP, Boyer N, Martinot-Peignoux M, Valla D, Vidaud M, Marcellin P: **Liver gene expression signature to predict response to pegylated interferon plus ribavirin combination therapy in patients with chronic hepatitis C.** *Gut* 2008, **57(4)**:516-524.
16. Feld JJ, Nanda S, Huang Y, Chen W, Cam M, Pusek SN, Schweigler LM, Theodore D, Zacks SL, Liang TJ, Fried MW: **Hepatic gene expression during treatment with peginterferon and ribavirin: Identifying molecular pathways for treatment response.** *Hepatology* 2007, **46(5)**:1548-1563.
17. Chen L, Borozan I, Feld J, Sun J, Tannis LL, Coltescu C, Heathcote J, Edwards AM, McGilvray ID: **Hepatic gene expression discriminates responders and nonresponders in treatment of chronic hepatitis C viral infection.** *Gastroenterology* 2005, **128(5)**:1437-1444.
18. Tanaka Y, Nishida N, Sugiyama M, Kurosaki M, Matsuura K, Sakamoto N, Nakagawa M, Korenaga M, Hino K, Hige S, Ito Y, Mita E, Tanaka E, Mochida S, Murawaki Y, Honda M, Sakai A, Hiasa Y, Nishiguchi S, Koike A, Sakaida I, Imamura M, Ito K, Yano K, Masaki N, Sugauchi F, Izumi N, Tokunaga K, Mizokami M: **Genome-wide association of IL28B with response to pegylated interferon-alpha and ribavirin therapy for chronic hepatitis C.** *Nature genetics* 2009, **41(10)**:1105-1109.
19. Younossi ZM, Baranova A, Afendy A, Collantes R, Stepanova M, Manyam G, Bakshi A, Sigua CL, Chan JP, Iverson AA, Santini CD, Chang SY: **Early gene expression profiles of patients with chronic hepatitis C treated with pegylated interferon-alfa and ribavirin.** *Hepatology* 2009, **49(3)**:763-774.
20. Dudoit S, Fridlyand J: **A prediction-based resampling method for estimating the number of clusters in a dataset.** *Genome Biol* 2002, **3(7)**: RESEARCH0036.
21. Dudoit S, Fridlyand J: **Bagging to improve the accuracy of a clustering procedure.** *Bioinformatics* 2003, **19(9)**:1090-1099.
22. **National Institutes of Health Consensus Development Conference Statement: Management of hepatitis C: 2002–June 10-12, 2002.** *Hepatology* 2002, **36(5 Suppl 1)**:S3-20.
23. Ferenci P, Fried MW, Shiffman ML, Smith CI, Marinos G, Goncales FL, Haussinger D, Diago M, Carosi G, Dhumeaux D, Craxi A, Chaneac M, Reddy KR: **Predicting sustained virological responses in chronic hepatitis C patients treated with peginterferon alfa-2a (40 KD)/ribavirin.** *J Hepatol* 2005, **43(3)**:425-433.
24. Sonkoly E, Stahle M, Pivarcsi A: **MicroRNAs and immunity: novel players in the regulation of normal immune function and inflammation.** *Seminars in cancer biology* 2008, **18(2)**:131-140.
25. Lindsay MA: **microRNAs and the immune response.** *Trends in immunology* 2008, **29(7)**:343-351.
26. Chen PY, Manninga H, Slanchev K, Chien M, Russo JJ, Ju J, Sheridan R, John B, Marks DS, Gaidatzis D, Sander C, Zavolan M, Tuschl T: **The developmental miRNA profiles of zebrafish as determined by small RNA cloning.** *Genes & development* 2005, **19(11)**:1288-1293.
27. Peng X, Li Y, Walters KA, Rosenzweig ER, Lederer SL, Aicher LD, Proll S, Katze MG: **Computational identification of hepatitis C virus associated microRNA-mRNA regulatory modules in human livers.** *BMC Genomics* 2009, **10**:373.
28. Gong AY, Zhou R, Hu G, Li X, Splinter PL, O'Hara SP, LaRusso NF, Soukup GA, Dong H, Chen XM: **MicroRNA-513 regulates B7-H1 translation and is involved in IFN-gamma-induced B7-H1 expression in cholangiocytes.** *J Immunol* 2009, **182(3)**:1325-1333.
29. Yu D, Rao S, Tsai LM, Lee SK, He Y, Sutcliffe EL, Srivastava M, Linterman M, Zheng L, Simpson N, Ellyard JI, Parish IA, Ma CS, Li QJ, Parish CR, Mackay CR, Vinuesa CG: **The transcriptional repressor Bcl-6 directs T follicular helper cell lineage commitment.** *Immunity* 2009, **31(3)**:457-468.
30. Hsu PW, Lin LZ, Hsu SD, Hsu JB, Huang HD: **ViTa: prediction of host microRNAs targets on viruses.** *Nucleic acids research* 2007, **35(Database issue)**:D381-385.
31. Pulendran B, Tang H, Denning TL: **Division of labor, plasticity, and crosstalk between dendritic cell subsets.** *Curr Opin Immunol* 2008, **20(1)**:61-67.
32. Wertheimer AM, Bakke A, Rosen HR: **Direct enumeration and functional assessment of circulating dendritic cells in patients with liver disease.** *Hepatology* 2004, **40(2)**:335-345.
33. Dienstag JL, McHutchison JG: **American Gastroenterological Association technical review on the management of hepatitis C.** *Gastroenterology* 2006, **130(1)**:231-264.

Pre-publication history

The pre-publication history for this paper can be accessed here:
http://www.biomedcentral.com/1755-8794/3/48/prepub

doi:10.1186/1755-8794-3-48
Cite this article as: Murakami *et al.*: Hepatic microRNA expression is associated with the response to interferon treatment of chronic hepatitis C. *BMC Medical Genomics* 2010 **3**:48.

Pathology International

Pathology International 2010; **60**: 351–357 doi:10.1111/j.1440-1827.2010.02526.x

Original Article

Deregulation of miR-92a expression is implicated in hepatocellular carcinoma development

Masatoshi Shigoka,[1] Akihiko Tsuchida,[1] Takaaki Matsudo,[1] Yuichi Nagakawa,[1] Hitoshi Saito,[1] Yoshiaki Suzuki,[1] Tatsuya Aoki,[1] Yoshiki Murakami,[2] Hidenori Toyoda,[3] Takashi Kumada,[3] Ralf Bartenschlager,[4] Nobuyuki Kato,[5] Masanori Ikeda,[5] Tomoki Takashina,[6] Masami Tanaka,[6] Rieko Suzuki,[6] Kosuke Oikawa,[7] Masakatsu Takanashi[6] and Masahiko Kuroda[6]

[1]*Third Department of Surgery and* [6]*Department of Molecular Pathology, Tokyo Medical University, Tokyo, Japan,* [2]*Center for Genomic Medicine, Kyoto University, Kyoto, Japan,* [3]*Department of Gastroenterology, Ogaki Municipal Hospital, Ogaki, Japan,* [4]*Department of Infectious Diseases, Molecular Virology, University of Heidelbergand, Heidelberg, Germany,* [5]*Department of Tumor Virology, Okayama University Graduate School of Medicine, Okayama, Japan, and* [7]*First Department of Pathology, Wakayama Medical University, Wakayama, Japan*

MicroRNAs (miRNAs) belong to a class of the endogenously expressed non-coding small RNAs which primarily function as gene regulators. Growing evidence suggests that miRNAs have a significant role in tumor development and may constitute robust biomarkers for cancer diagnosis and prognosis. The *miR-17-92* cluster especially is markedly overexpressed in several cancers, and is associated with the cancer development and progression. In this study, we have demonstrated that miR-92a is highly expressed in hepatocellular carcinoma (HCC). In addition, the proliferation of HCC-derived cell lines was enhanced by miR-92a and inhibited by the anti-miR-92a antagomir. On the other hand, we have found that the relative amount of miR-92a in the plasmas from HCC patients is decreased compared with that from the healthy donors. Interestingly, the amount of miR-92a was elevated after surgical treatment. Thus, although the physiological significance of the decrease of miR-92a in plasma is still unknown, deregulation of miR-92 expression in cells and plasma should be implicated in the development of HCC.

Key words: hepatocellular carcinoma, microRNA, miR-638, miR-92a, plasma

Correspondence: Masahiko Kuroda, MD, PhD, Department of Molecular Pathology, Tokyo Medical University, 6-1-1 Shinjuku, Shinjuku-ku, Tokyo 160-8402, Japan. Email: kuroda@tokyo-med.ac.jp

Received 8 November 2009. Accepted for publication 23 December 2009.

MicroRNAs (miRNAs) are small endogenous non-coding RNAs that regulate gene expression and have a critical role in many biological and pathological processes.[1] Recent studies have shown that deregulation of miRNA expression contributes to the multistep processes of carcinogenesis, and have shown promise as tissue-based markers for cancer classification and prognostication.[2,3] However, biological roles of only a small fraction of known miRNAs have been elucidated to date.

The miR-17-92 cluster at 13q31.3 is consists of six miRNAs: miR-17, miR-18a, miR-19a, miR-20a, miR-19b-1 and miR-92a-1, and plays an important role for development of lung cancer,[4] B-cell lymphomas,[5] chronic myeloid leukemia,[6] medulloblastomas,[7] colon cancer[8] and hepatocellular carcinoma (HCC).[9] In addition, mice deficient in the miR-17-92 cluster died shortly after birth with lung hypoplasia, and B-cell development was impaired in the mice.[10] It has been reported, however, that miR-92a increases cell proliferation by negative regulation of an isoform of the cell-cycle regulator p63.[11] Furthermore, miR-92a regulates angiogenesis.[12] Thus, it is clear that the miR-92a has some oncogenic characteristics. However, the specific biological role of miR-92a in the processes of human cancer development has remained unclear.

Here, we have revealed that miR-92a is implicated in human HCC development. Furthermore, we have demonstrated that miR-92a in human blood has the potential to be a noninvasive molecular marker for diagnosis of human HCC.

MATERIALS AND METHODS

In situ hybridaization of miR-92a

Locked nucleic acid (LNA)-modified probes for miR-92a and negative control (miRCURY-LNA detection probe, Exiqon, Vedbaek, Denmark) were used. The probe sequences were as follows; *miR-92a*, 5′-ACAGGCCGGGACAAGTGCAATA-3′; and a scrambled oligonucleotides used for negative control, 5′-GTGTAACACGTCTATACGCCCA-3′. *In situ* hybridization was performed using the RiboMap *in situ* hybridization kit (Ventana Medical Systems, Tucson, AZ, USA) on the Ventana Discovery automated *in situ* hybridization instrument (Ventana Medical Systems). The *in situ* hybridization steps were performed as previously described.[13] Staining was evaluated by two investigators and graded as follows: negative (–), no or occasional (<5%) staining of tumor cells; positive (+), mild to strong (>5%) staining of tumor cells. Paraffin-embedded tissue samples of hepatocellular carcinoma (HCC) and adjacent non-tumorous liver cirrhosis (LC) were obtained from HCC patients at Ogaki Municipal Hospital (Ogaki, Japan). Details of the clinical data are provided in Table 1.

Plasma collection, RNA isolation and quantitative RT-PCR

Whole blood samples were collected from healthy donors and the patients with HCC at Ogaki Municipal Hospital. This study was approved by the institutional review board (IRB) of Tokyo Medical University, and all subjects provided written informed consent under the institutional review board. Details of clinical data are provided in Table 1. Diagnoses were confirmed using the post-operated tissues. Blood samples of the patients (Cases 1–10) were collected one day before the operation and then properly stored. One week after operation, blood samples of the patients were collected again. Whole blood was separated into plasma and cellular fractions by centrifugation at 1600 *g* for 15 min. Total RNA in the

Table 1 Summary of clinical details of hepatocellular carcinoma (HCC)used for in situ hybridaization and serum analysis

	Year	Sex	Virus type	Histologic type	Stage	Child-Pugh	miR-92a
Case 1	53	Male	HBV	Poorly	I	A	+
Case 2	59	Male	HBV	Moderate	II	A	+
Case 3	79	Male	NBNC	Moderate	III	A	+
Case 4	73	Male	HCV	Well	I	A	+
Case 5	76	Female	HCV	Moderate	IV-A	A	+
Case 6	59	Male	HCV	Moderate	II	A	+
Case 7	69	Female	HCV	Moderate	I	A	+
Case 8	71	Male	HCV	Moderate	I	A	+
Case 9	59	Female	HBV	Well	I	A	–
Case 10	69	Male	NBNC	Moderate	IV-A	A	–
Case 11	61	Female	HBV	Poorly	IV-A	B	+
Case 12	73	Male	NBNC	Moderate	II	A	+
Case 13	67	Male	NBNC	Moderate	IV-A	A	+
Case 14	61	Male	NBNC	Moderate	III	A	+
Case 15	45	Male	HBV	Moderate	I	A	+
Case 16	68	Female	HCV	Moderate	III	A	+
Case 17	70	Male	NBNC	Poorly	II	A	+
Case 18	59	Male	HCV	Moderate	III	A	+
Case 19	43	Male	HBV	Moderate	II	A	+
Case 20	69	Male	HCV	Moderate	II	A	–
Case 21	76	Male	HCV	Moderate	III	A	–
Case 22	53	Male	HCV	Moderate	II	A	–

HCV, hepatitis C virus; HBV, hepatitis B virus; NBNC, non-B non-C virus.

Table 2 Summary of clinical details of hepatocellular carcinoma (HCC) used for qPCR analysis

Code no.	Year	Sex	Virus type	Histologic type	Non-tumorous tissue	AFP	PIVKA-II
91	53	Male	HCV	Moderate	LC	5	0.06
160	59	Male	HCV	Moderate	LC	NI	NI
O89	68	Male	HCV	Moderate	LC	8	25
O90	70	Male	HCV	Moderate	LC	686	962
K89	51	Male	HCV	Moderate	LC	NI	NI

LC, liver cirrhosis; HCV, hepatitis C virus; NI, no information.